Luís Miguel Pereira Domingues Alho

Licenciatura em Ciências de Engenharia Biomédica

Automated quantitative analysis of MCC-IMS spectra

Dissertação para obtenção do Grau de Mestre em
Engenharia Biomédica

Orientador: Valentina Vassilenko, Professor Auxiliar, Faculdade de Ciências e Tecnologia da Universidade Nova de Lisboa

Co-Orientador: André Damas Mora, Professor Auxiliar, Faculdade de Ciências e Tecnologia da Universidade Nova de Lisboa

Júri:

Presidente: Doutora Carla Maria Quintão Pereira

Arguente: Doutor Pedro Manuel Cardoso Vieira

Vogais: Doutora Valentina Vassilenko

FACULDADE DE
CIÊNCIAS E TECNOLOGIA
UNIVERSIDADE NOVA DE LISBOA

Setembro, 2014

Automated quantitative analysis of acetone and isoprene of MCC-IMS spectra

Agradecimentos

Esta tese representa não só a conclusão de um trabalho mas também a conclusão de toda uma etapa da minha vida, assim gostaria de agradecer a várias pessoas que tornaram isto possível.

Aos meus orientadores, Valentina Vassilenko e André Mora, pela informação e conhecimento transmitido, assim como toda a paciência e dedicação que tiveram para comigo ao longo deste trabalho.

À minha mãe por todo o apoio que me dá e por querer sempre o melhor para mim. Ao meu pai por todos os conselhos que me deu ao longo da minha vida e que moldaram quem sou. Ao meu avô Amílcar por ser o meu exemplo de vida e pela sua dedicação aos seus netos. À minha avó Cecília por todo o carinho que sempre me deu. Aos meus irmãos, João e Catarina, por alegrarem a minha vida sempre que estou com eles e para os quais espero ser um bom exemplo.

Abstract

Ion Mobility Spectrometry coupled with Multi Capillary Columns (MCC -IMS) is a fast analytical technique working at atmospheric pressure with high sensitivity and selectivity making it suitable for the analysis of complex biological matrices.

MCC-IMS analysis generates its information through a 3D spectrum with peaks, corresponding to each of the substances detected, providing quantitative and qualitative information. Sometimes peaks of different substances overlap, making the quantification of substances present in the biological matrices a difficult process.

In the present work we use peaks of isoprene and acetone as a model for this problem. These two volatile organic compounds (VOCs) that when detected by MCC-IMS produce two overlapping peaks. In this work it’s proposed an algorithm to identify and quantify these two peaks. This algorithm uses image processing techniques to treat the spectra and to detect the position of the peaks, and then fits the data to a custom model in order to separate the peaks. Once the peaks are separated it calculates the contribution of each peak to the data.

Keywords: Ion Mobility Spectrometry (IMS); Multicapillary columns (MCC); Image Processing; Volatile Organic Compounds (VOCs); Quantification; Surface fitting

Resumo

A espectroscopia de mobilidade iónica (IMS) acoplada a Colunas Multicapilares (MCC) é uma técnica analítica rápida, que funciona a pressão atmosférica, com alta sensibilidade e alta selectividade tornando-a ideal para a análise de matrizes biológicas de alta complexidade.

A MCC-IMS gera informação sobre a forma de um espectro 3D. Este espectro fornece informação qualitativa e quantitativa na forma de picos, correspondentes a cada substância. No entanto estes picos por vezes aparecem sobrepostos dificultando a sua quantificação.

Neste trabalho utilizamos os picos de isopreno e acetona como modelo para este problema. Estes dois compostos voláteis orgânicos quando detectados pela MCC-IMS geram dois picos que se sobrepõem. É proposto neste trabalho um algoritmo para quantificar estas duas substâncias. Este algoritmo utiliza técnicas de processamento de imagem para tratar os espectros e para detectar a posição dos picos. Após a detecção destes picos o algoritmo ajusta um modelo personalizado aos dados do espectro de maneira a se poder separar os picos. Uma vez separados os picos calcula a contribuição de cada pico no espectro.

Palavras-chave: Espectroscopia Mobilidade Iónica (IMS); Colunas Multicapilares (MCC); Processamento de Imagem; Compostos voláteis Orgânicos (VOCs); Quantificação; Surface fitting**;**

Contents

AGRADECIMENTOS I

ABSTRACT III

RESUMO V

CONTENTS VII

TABLES IX

FIGURES XI

ABBREVIATIONS XIII

1. INTRODUCTION 1

1.1. Outline 3

2. THEORY 5

2.1. Ion Mobility Spectrometry 5

2.1.1. Working Principles 5

2.1.2. Spectrometer Components 6

2.2. Multi Capillary Columns Coupling 7

2.3. Spectrum 8

3. STATE OF ART OF SPECTRA ANALYSIS 11

3.1. De-noising and Smoothing 11

3.1.1. Moving Average Filter 11

3.1.2. Savitzky-Golay Filter 11

3.1.3. State of Art 12

3.2. Curve Fitting 12

3.3. RIP detailing 13

3.4. Peak Detection 14

3.4.1. Merged Peak Cluster Localization 14

3.4.2. Growing Interval Merging 14

3.4.3. Wavelet-Based Multiscale Peak Detection 15

3.4.4. Watershed Transformation 15

3.5. Peak Modeling 16

4. METHODS 17

4.1. Process 17

4.2. Data Filtering 17

4.3. RIP Detailing 18

4.4. Region of Interest 22

4.5. Spectral peak detection 24

4.6. Spectral peaks modeling 25

5. RESULTS OF PEAK ANALYSIS 29

5.1. Peak Detection 29

5.2. Fit 32

5.3. Peak Volumes 35

6. CONCLUDING REMARKS 37

6.1. Future Work 38

BIBLIOGRAPHY 39

APPENDIX A 41

APPENDIX B 47

APPENDIX C 49

Tables

Table 4.1 - Initial parameters of lognormal curve and their upper and bottom bounds 20
Table 4.2 - Initial parameters of lognormal curve and their upper and bottom bounds 20
Table 4.3 - Analysis of the empiric detection of acetone peak 22
Table 4.4 - Analysis of the empiric detection of isoprene peak 22
Table 4.5 - Analysis of the empiric region of interest 23
Table 4.6 - Initial parameters and their upper and lower bounds for the peaks model 27
Table 5.1 - Results of the acetone peak detection 29
Table 5.2 - Results of the isoprene peak detection 30
Table 5.3 - Parameters of the each individual peak 33

Figures

Figure 2.1 - A model of an IMS tube and its working principle 6
Figure 2.2 - A multi capillary column 7
Figure 2.3 - Pseudo color representation of IMS data 8
Figure 2.4 - A Topografic view of a MCC-IMS spectrum and a single spectrum line 9
Figure 2.5 - Example of a 2D fitting process to a MCC-IMS spectrum 10
Figure 3.1 - Before and after RIP detailing by subtracting the detailing function 13
Figure 4.1 - Results of different filters applied in a single line spectrum 18
Figure 4.2 - Result of the rip detailling 21
Figure 4.3 - Example of the region of interest selection 23
Figure 4.4 - Peak detection algorithm example 24
Figure 5.1 - Acetone peaks distribution 30
Figure 5.2 - Isoprene peaks distribution 31
Figure 5.3 - Result of the fit 32
Figure 5.4 - Acetone peak isolated 33
Figure 5.5 - Third peak isolated 34
Figure 5.6 - Isoprene peak isolated 34
Figure 5.7 - Example of a bad fit 35

Abbreviations

E	Electric Field
GIM	Growing Interval Merging
GPL	Gradient Path Labeling
IMS	Ion Mobility Spectrometry
K	Ion Mobility
K_0	Reduced Ion Mobility
MCC	Multicapillary Columns
MPCL	Merged Peak Cluster Localization
RIP	Reactant Ion Peak
ROI	Region Of Interest
tDrift	Drift Time
tRet	Retention Time
v_d	Ion Velocity
VOCs	Volatile Organic Compounds
WBMPD	Wavelet-Based Multiscale Peak Detection
WST	Watershed Transformations

1. Introduction

Ion Mobility Spectrometry is a recent analytical technique for the detection of gas-phase analytes. Because its operation does not require vacuum, IMS is seen as one of the most promising techniques for gas spectrometry.

Developed during 1970's it was initially used for military purposes [**1**]. Initially seen as a niche technology, without much room for improvement, its development slowed down and the technique turned into a rejected method. This rejection occurred due to the lack of understanding of the principles of ion molecule chemistry and ion behavior at atmospheric pressure. In the 90's refinements in the IMS instrumentation expanded the capabilities of the technique, becoming a general-purpose technology [**2**]. The coupling of IMS with multi capillary columns (MCC) increased the technique selectivity without resorting to pre-separation techniques.

This combination brought new possible applications for the technique, being the detection of volatile organic compounds (VOCs) one of the most interesting and promising applications. Volatile organic compounds are organic chemicals that possess low boiling point and so evaporate at ambient temperatures. These compounds have numerous origins, including biological and anthropogenic sources. VOC monitoring has numerous applications, some of them can be harmful to human health while others can be indicators of biological processes, like the detection of Dyacetyl in beer fermentation, quality control of food, and detection of marker substances in human breath [**3**]. Isoprene and acetone are two VOCs that, due to their characteristics, appear in the IMS spectra in close positions and because they have some relevance in the metabolic profiling, medical diagnosis and therapy monitoring will be studied in this work.

Acetone ($(CH_3)_2$ CO) is an organic compound widely used as a solvent in the industry. It has a molar mass of 58.08 $g\ mol^{-1}$ and its boiling point is between 56ºC and 57ºC in standard conditions, making it a high volatile substance. In ambient conditions is a highly flammable liquid with a characteristic odor. It's also a compound produced in the human body as part of the breakdown and utilization of fats and lipids. The earliest report of acetone related to a human pathology dates 1798 described as an "odor of decaying apples" by John Gallo. More recent studies have found relationships between the concentrations of acetone in breath and diabetes (e.g. in human breath acetone at a concentration of 400 *ppb* is normal but at 1000-1200 *ppb* can be an indicator for diabetes). Also correlations of the concentration of acetone in breath and exercise intensity have been found [**4**] [**5**].

Isoprene (C_5H_8) is another organic compound with a molar mass of 68.12 $g\ mol^{-1}$ and its boiling point is 34º*C* in standard conditions. Possesses high volatility and it's produced by all kinds of living organisms, including human beings. Like Acetone, it's always present in the human breath and variations of its concentration levels can be used as an indicator of health and disease. Although no conclusive results have been taken isoprene levels are believed to be a good additional indicator to metabolic disorders and also in cancer screening [**6**] [**7**] [**8**].

The MCC-IMS spectrum is a 3D matrix that contains the information of the detected substances as peaks. The position of these peaks in the spectrum gives qualitative information of the detected substances. Resorting to automatic methods to detect peaks and, subsequently, using statistical analysis, correlation between a peak position and what substance it represents can be achieved. There is also the possibility to extract quantitative information from these peaks.

The need for the extraction of quantitative information arises from necessity to identify changes in the quantity of the substances detected, these changes are vital to characterize certain biological processes. Isoprene and Acetone are two substances represented in the MCC-IMS spectrum in positions near one from the other, creating overlapping peaks. Overlapping peaks are hard to quantify due to their addictive contributions. A method to correctly deconvolute these peaks is needed in order to quantify both substances. In this work the development of an algorithm to identify and quantify the acetone and isoprene peaks is proposed.

1.1.Outline

This thesis is organized in 6 main chapters. **Chapter 1** is the introduction, where the theme of this thesis is introduced. **Chapter 2** is comprised of the IMS-MCC details, giving an idea of the physical background, the resulting data and its associated problems. In **Chapter 3** the current state of art techniques used in the IMS-MCC data are presented. In **Chapter 4** all the methods used in this work are explained as well as the justifications of the choices made throughout the work. **Chapter 5** contains the analysis of the data obtained as result of this work. **Chapter 6** is where the final conclusions of this work are made and proposals of future work are given. This work also has two appendixes. **Appendix A** contains a series of results achieved with the algorithm presented in this thesis. **Appendix B** contains the poster accepted and exposed in the 8th International Conference on Breath Research & Cancer Diagnosis. **Appendix C** is the certificate of presence as a speaker in the JORTEC 2014.

2. Theory

2.1.Ion Mobility Spectrometry

2.1.1. Working Principles

IMS is based on a simple principle, ions created at normal pressure move in the direction established by an external electrical field against the direction of a carrier gas. IMS ionizes gaseous analytes and then extracts the information of their characteristic drift time. The ions drift time is characteristic because their mass and/or structure make them attain different velocities in the drift gas [**9**] [**10**]. Due to the relation between the ion velocity and the intensity of an applied external electric field an independent component for each ion can be extracted. This component is the quotient between ion velocity (v_d) and Electric field (E) and is referred as ion mobility (K).

$$K = \frac{v_d}{E} \qquad 2.1$$

Ion velocity is expressed in cm^2s^{-1} and the electric field is in Vcm^{-1} therefor the ion mobility is expressed in $cm^2V^{-1}s^{-1}$. Due to the physical laws of our universe, ion mobility is susceptible to both temperature and pressure. This susceptibility required a correction in order assure stable results. By normalizing to the standard temperature and pressure we get the reduced ion mobility (K_0).

$$K_0 = K\left(\frac{P}{P_0}\right)\left(\frac{T_0}{T}\right) \qquad 2.2$$

Where P and T are the values of pressure and temperature during the experiment. This means that the reduced ion mobility constant (K_0) is a substance-specific value.

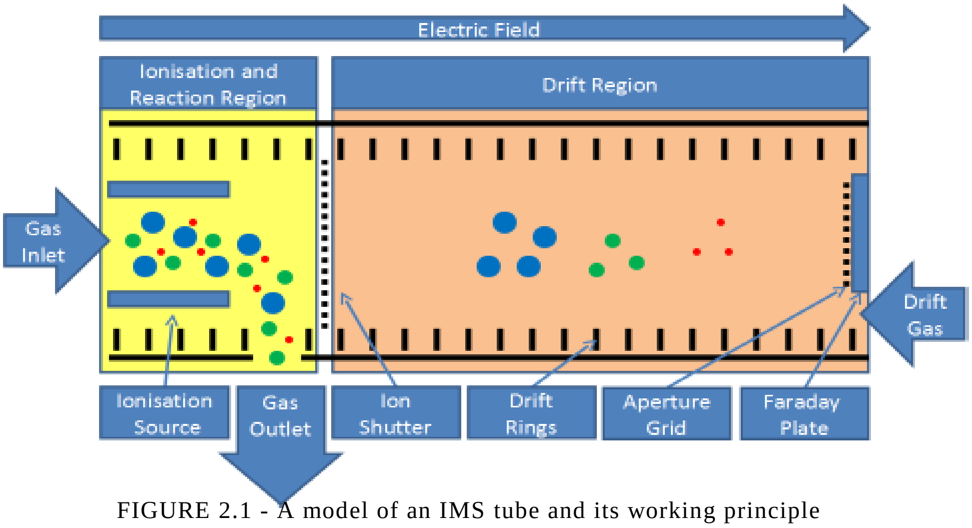

FIGURE 2.1 - A model of an IMS tube and its working principle

An ion mobility spectrometer is comprised of a series of components. Usually the spectrometer main components are a drift tube, a sample inlet, a high voltage supply, a shutter grid, an amplifier, a drift gas supply, pressure and temperature sensors, and a computer.

The drift tube is the main component of the spectrometer. Two entrances (the inlet sample and the drift air entrance), an exhaust exit, a Faraday detector, a shutter grid, a radiation source, drift rings and an aperture grid are the elements present in the tube. Divided by the shutter grid two regions exist, the ionization region and the drift region.

In the ionization region the radiation source forms positive and negative ions. Because these ions are reactant the sample molecules undergo ion molecules reactions forming product ions. Opening the shutter grid for a moment allows the product ions to get into the drift region. An electric field is applied on the product ions. These ions migrate against the drift gas due to the electric field. Since the ions possess different masses and/ or structure, they reach the Faraday plate at different times. The different signals generated by the detector are recorded in the ion mobility spectrum, giving information on the different drift times (ms) and their respective intensity.

2.1.2. Spectrometer Components

The tube is usually made of metal rings separated by isolators. The high-voltage supply (±1-10 *kV*) creates an electric field inside the tube with field gradients from 150 to 300 *V/cm*. Their design depends on the ionization source selected. Presently the know sources for IMS include radiation sources (α and β radiation), UV lamps, lasers, different kinds of discharges, and electrospray ionization [**2**]. The most common β radiation source is ^{63}Ni although Tritium can also be used for some applications.

The shutter grid works by creating an additional field gradient that is perpendicular to the one of the measuring tube not allowing the ions to pass. When the field is turned off the ions can pass through the grid.

For the purpose of getting better mobility spectra an aperture grid is positioned in front of the detector. It provides a capacitive decoupling between arriving ions and the detector resulting in a mall line width of the peaks in the spectra.

2.2.Multi Capillary Columns Coupling

Multi capillary columns consist of various capillaries (around 1000) all bundled into a single tube with a typical diameter of 3 *mm*. Their function is to separate complex mixtures, while offering high flow rate and a high sample capacity when compared to single narrow bow columns [**11**].

Because the ion mobility spectrometer does not have a very high selectivity, there is the need to be coupled with MCC. MCC offers a high carrier gas flow which enables an isothermal separation of VOCs at ambient temperatures. Thus, because of the high capacity, favorable flow conditions, and low working temperatures, MCC is ideal to be coupled with IMS, assuring that the equipment does not have to increase in size.

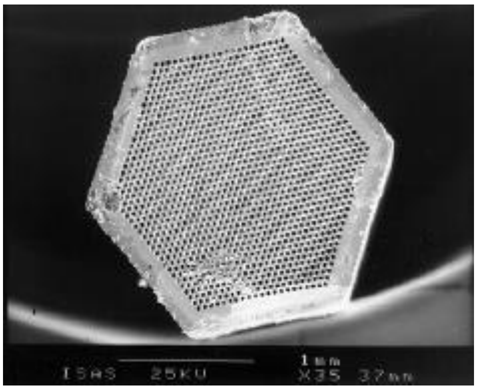

FIGURE 2.2 - A multi capillary column

The IMS-MCC coupling also enables a multidimensional data analysis, allowing identification of VOCs by both chromatographic data (retention times) and by the ion mobility data. The multidimensional data analysis also allows the distinction of monomers, dimers and trimmers of certain molecules.

2.3.Spectrum

The spectrum generated by the IMS-MCC spectrometer is a 3 dimensional plot.

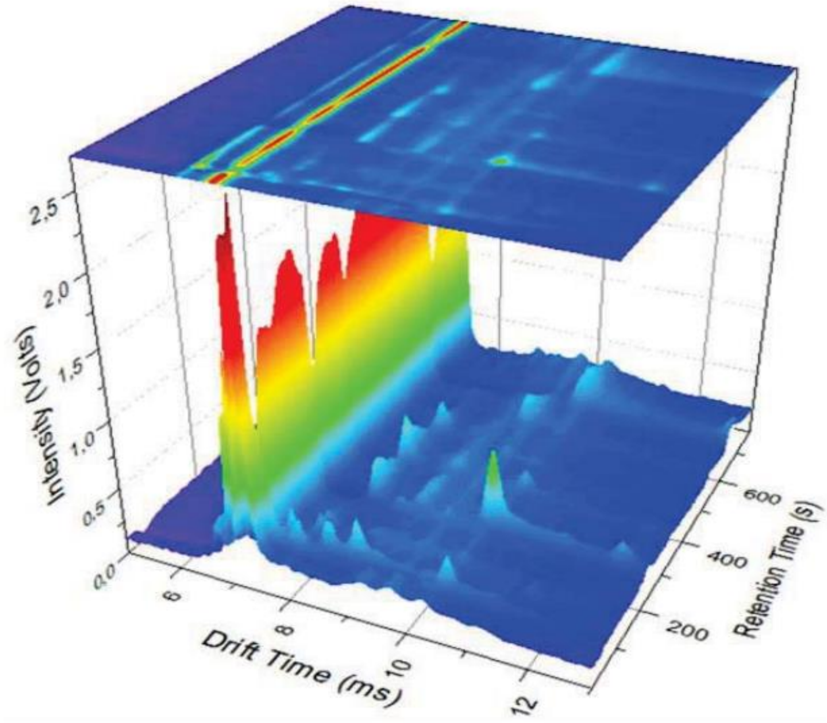

Figure 2.3 - Pseudo color representation of IMS data

The drift time is in the x-axis, the retention time is in the y-axis, and the intensity of the signal from the Faraday plate is in the z-axis. This data can be plotted in topographic view with the intensity being color-coded, which allows easy pattern detection, crucial for the detection of VOCs.

An IMS spectrum has one characteristic peak that appears in all spectra. It's called the reactant ion peak (RIP) and its descent signal is called the RIP tailing. The RIP is formed by the ionization of the carrier drift gas. If there are no molecules detected the RIP has the maximum amount of ions, this means that in zone where a molecule is detected the RIP decreases in size. This phenomenon occurs because the product ions of the sample molecules are made by the collisions of reactant ions and sample molecules [**2**].

Each substance has a specific peak due to its reduced ion mobility constant. However, when multiple substances are analyzed, some peaks can overlap. When peaks are overlapped they give cumulative contributions to the spectrum. For a precise quantification of substances peaks the different contributions need to be isolated.

Figure 2.4 is an example of a simple IMS spectrum. It will be used to explain the profile of a peak and its characteristics.

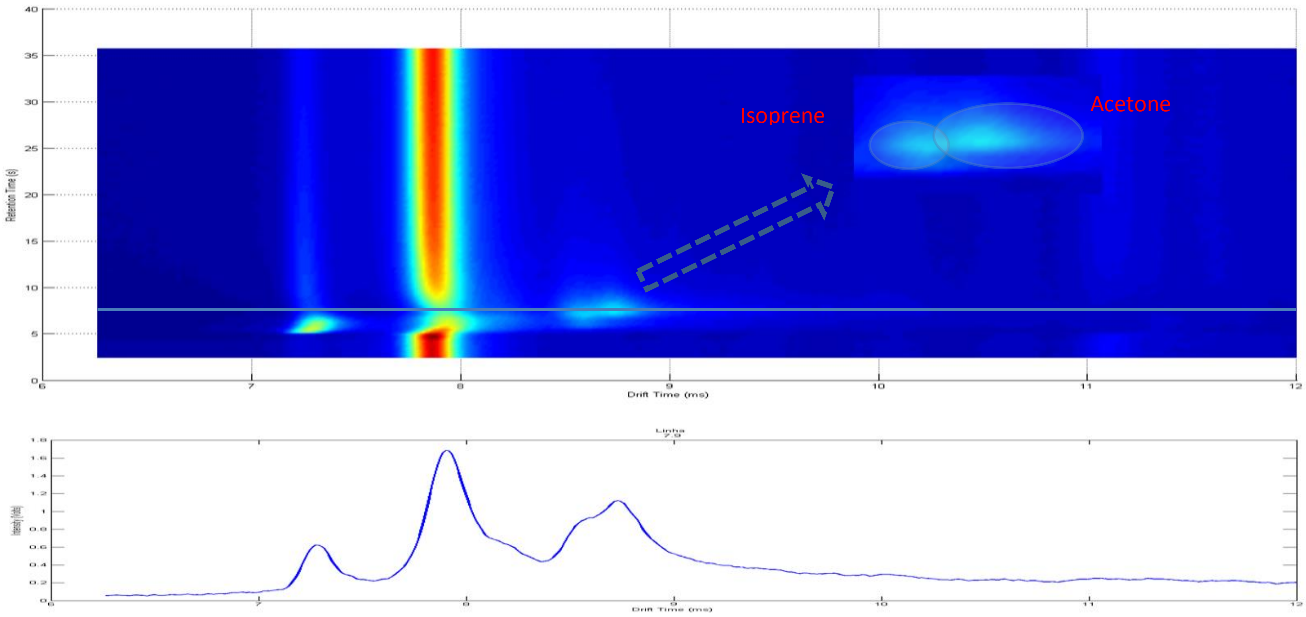

Figure 2.4 - A Topografic view of a MCC-IMS spectrum and a single spectrum line

First the peaks need to be characterized A process of fitting is to be applied to modulate these peaks. This process allows an easier analysis of the complexities of the spectrum. After the identification of the individual peaks’ characteristics, a correlation between these characteristics and the concentration of substance can be achieved.

Figure 2.4 is an example of two overlapped peaks (Isoprene and Acetone). Using a side view we can observe the peaks profile, allowing a better understanding of what shape each peak has. The peaks seem to exhibit the shape of a Gaussian curve with a tailing in the direction of the drift time. They are also standing on top of a baseline curve. To isolate the “real” values of the peaks, they need to be isolated. First the peaks need to be characterized and a model created. Then a process of fitting is to be applied to find the parameters that best represent the data in the model. This process allows for an easier analysis of the complexities of the spectrum their corresponding contributions. After the identification of the individual characteristics of peaks, a correlation between these characteristics and the concentration of substance can be achieved.

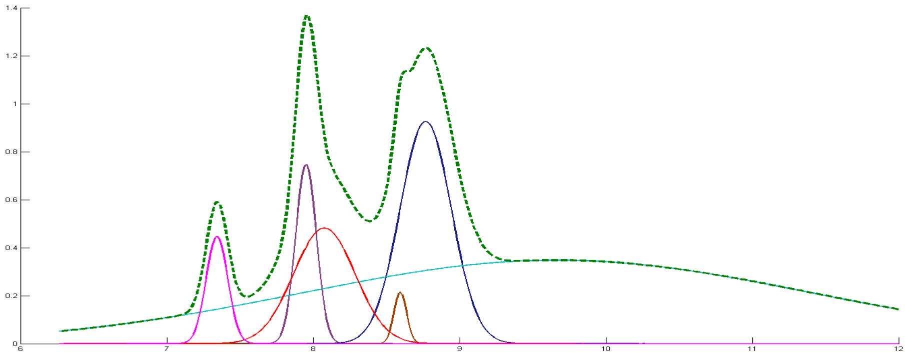

Figure 2.5 - Example of a 2D fitting process to a MCC-IMS spectrum

3. State of Art of Spectra Analysis

In the scope of quantitative analysis of IMS spectra, this section presents the current techniques for IMS spectra data analysis. These methods provide the necessary tools to treat the data in a way that the peaks deconvolution can be achieved.

3.1.De-noising and Smoothing

Like most spectra, MCC-IMS spectra contains noise. This noise makes it difficult to detect low intensity signals. The process of de-noising and smoothing the data allows the reduction or the enhancement of certain aspects of the data. However this process can lead to loss of crucial information. This means that there is the need to find a filter that produces negligible loss of information and still maintain the important aspects of the data. The characteristics of the noise and the data influence the choice of the filter. The following sections present some filtering techniques.

3.1.1. Moving Average Filter

The Moving average filter is a filter that evaluates the average value on a determined window focused on each point of a data set. Although it is very fast filter to compute, it does not distinguish data and noise very effectively, leading to strong attenuations of the data and loss of important information.

3.1.2. Savitzky-Golay Filter

The Savitzky-Golay filter is a digital filter proposed by Savitzky et al. in 1964 [**12**]. The filter possesses 2 adjustable parameters, the window size and the polynomial degree. This filter is very effective in reducing the noise and maintaining the shape and height of waveform peaks [**13**]. The filter works by splitting the data in samples (window size determines the size of this samples) then a linear regression of some polynomial individually for each sample, followed by the evaluation of that polynomial exactly at the very position of the sample [**14**].

3.1.3. State of Art

Wavelet transforms were used by Bader et al. 2008 [**15**]. Applied to different levels of resolutions these wavelet transforms achieved both de-noising and smoothing. Removing low amplitude coefficients resulted in de-noising. Removing the coefficients corresponding to high frequency regions resulted in smoothing of the data.

Bunkowski used a combination of filters to achieve de-noising [**16**]. A median filter followed by a Gaussian filter. The median filter is used to eliminate single noise fragments and the Gaussian filter to smooth the remaining values.

3.2. Curve Fitting

Curve Fitting is the process of finding a curve that best fits a certain data set. This curve or mathematical equation allows for a better visualization and a better analysis of the data. Two things are needed for this process, a model that can describe the data and a method that can find the ideal parameters for the model. The fitting process can require a lot of computation time, depending on the size of the data and the number of parameters that needs to calculate.

For the purpose of this thesis the Levenberg-Marquardt method is going to be used. This method is used to solve Non-linear least squares problems, being essentially a search method used for non-linear regressions. It searches for the ideal parameters that solve non-linear regression problems. It is based in the Gauss-Newton method because it evaluates partial derivatives to ascertain the direction of the search, but contrary to the

Gauss-Newton method it possesses the ability to create boundaries to the parameters that solved the non-linear regression problem.

3.3.RIP detailing

A characteristic signal structure is found in all MCC-IMS spectra, the reactant ion peak (RIP). To facilitate analysis there is the need to eliminate this peak. This process is called RIP detailing.

In 2008 Bader *et al.* achieved RIP detailing by fitting a modified lognormal function (3.1), where θ is the shift in the x axis, σ defines the shape of the curve, and μ is the log scale, to the mean of all spectra and then subtracting the fitted function from each spectrum [**15**].

$$L(x_i) = \frac{a_d}{(x_i - \theta)\sigma\sqrt{2\pi}} \cdot exp\left[-\frac{[\log((x_i - \theta) - \mu)]^2}{2\sigma^2}\right] \qquad 3.1$$

This lognormal function met the general assumption of Gaussian peaks and the right screwed shape of the RIP tailing.

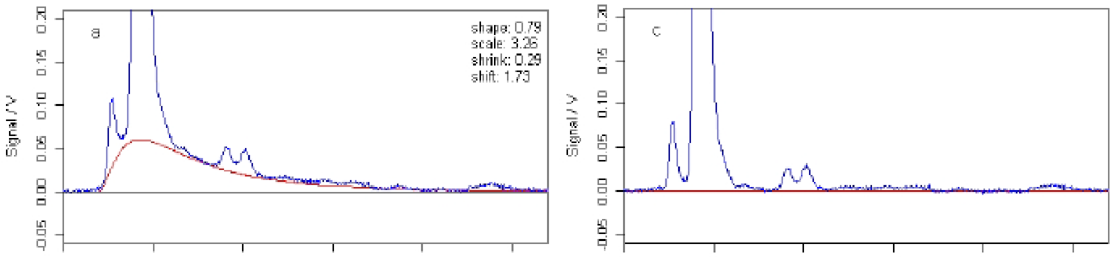

Figure 3.1 - Before and after RIP detailing by subtracting the detailing function

More recently, Bunkowski proposed a method where an ascending sorted list with all the values with the same $1/K_0$ value is created [**16**]. Then, the 25% quantile of every $1/K_0$ is selected and subtracted over all spectra. This method removes the RIP and corrects the baseline.

3.4.Peak Detection

Both Bader and Bunkowski presented different approaches to detect peaks in IMS data. Bader introduced three different methods, the Merged Peak Cluster Localization (MPCL), the Growing Interval Merging (GIM), and the Wavelet-Based Multiscale Peak Detection (WBMPD) [**15**]. Bunkowski introduced an algorithm based on Watershed Transformations (WST) [**16**].

3.4.1. Merged Peak Cluster Localization

This method instead of utilizing a preprocessing baseline correction, it uses a LOWESS algorithm [**17**]. LOWESS is a robust locally weighted regression method that was used to reduce the RIP tailing and mitigate the signal noise. After the LOWESS algorithm is applied the data is the data is truncated after the RIP. This truncated data is then classified into two types, peaks and noise by k-means clustering. Finally a merging algorithm is applied to group the adjacent data points that were classified as peaks. Although some positive results were achieved, an important limitation of the method is its inability to detect superimposed peaks.

3.4.2. Growing Interval Merging

This method was developed to overcome the limitations of the MPCL method [**15**]. It starts by defining a sequence of intensity thresholds that characterize the growing intensity intervals. A histogram of the intensity is used to define these thresholds that divide the data in three regions, noise, peak, and RIP. The peak region is divided into subintervals with evenly distributed data points. Then a similar procedure to the MPCL is employed to each subinterval. This process allowed distinction between peak and non-peak and also different peak regions could be identified. An ellipse shape was chosen for each peak for the purpose of storing the peak information with minimal parameters. To detect overlapping peaks the GIM method was structured in a stage wise manner. In each stage a list is created with the peaks detected. If in the next stage a common peak is found the old peak parameters are overridden by the new parameters. Although the GIM outperforms the MPCL, there are still limitations in the detection off overlapping peaks.

3.4.3. Wavelet-Based Multiscale Peak Detection

This method is based on the approach by Randolph and Yasui for multiscale processing of single spectra [**18**] but applied to three-dimensional spectra. A maximal overlap discrete wavelet transform (MODWT) to perform multiple resolution analysis is used. This wavelet transform is translation invariant and can be applied to arbitrary data dimensions. A Haar wavelet yield better results. The wavelet transform produces four matrices with information of the data, the lowpass-lowpass (LL), the lowpass-highpass (LH), the highpass-highpass (HH), and the highpass-lowpass (HL). For the IMS data the LH matrices provided the necessary information for peak localization. Bader *et al.* applied the GIM method to the LH matrix to detect the peaks and extract their information. This method proved to be highly sensitive and provided better results than the standalone GIM method.

3.4.4. Watershed Transformation

Bunkowski proposed this method based on the work of Wegner et al. for the detection of spots in gel electrophoresis images. The concept of WST is by analyzing *the data as a topological permeable map which is submerged into an imaginary water basin* [**16**]. The IMS data is inverted so that the peaks reach the water first. The water starts filling the peaks until the data is fully immersed. When water from different peaks meet, a dam is built. This process partitions the data into regions separated by dams, called watersheds.

3.5.Peak Modeling

Kopcynski, Baumbach and Rahmann proposed a model for the IMS peaks [**19**]. This model is an inverse Gaussian distribution. While the original inverse Gaussian has its origin at zero the proposed model has an additional offset parameter, this means a

$$g_{\mu,\lambda,o}(x_i) = [x > o] \cdot \sqrt{\frac{\lambda}{2\pi(x-o)^3}} \cdot \exp\left[-\frac{\lambda\left((x-o)-\mu\right)^2}{2\mu^2(x-o)}\right] \tag{3.2}$$

total of three parameters are needed. Although there is no physical theory to describe the peaks observed this model possesses similar characteristics to the observed peaks. The ability to represent the data in a mathematical model and a series of parameters for each peak requires less space than saving millions of data points.

4. Methods

4.1.Process

In order to extract the quantitative information of Isoprene and Acetone peaks from the IMS spectra data, a methodology had to be applied.

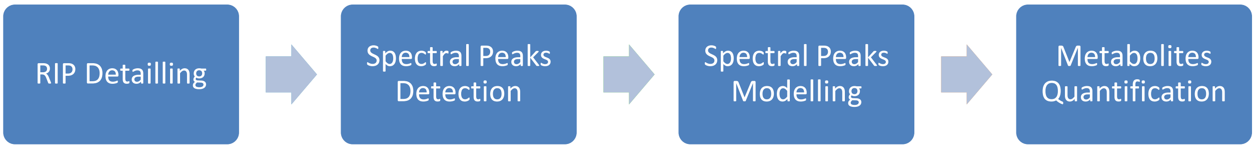

To reduce noise and fix data irregularities, a filter is applied in order to enhance the aspects of interest and improve the ensuing methods of the algorithm. Then, the RIP tailing is detected using 2D fitting and then subtracted, followed by the segmentation algorithm (described later on) applied in a specific area in order to detect the number of peaks and its position. Once the necessary information is collected a 3D fitting using the defined peak model is applied to achieve a representation of the data can be used to deconvolute the peaks and allow their quantification.

4.2.Data Filtering

The first step in the methodology was to apply a smoothing filter to reduce the noise influence. The filter was chosen considering the MCC-IMS spectra data, i.e. containing overlapping peaks.The filter had to be able to reduce the noise without significant changes to the shape of the peak curves.

The Savitzky-Golay filter is the filter widely used in the literature and in the industry, with proven results in this type of data. This filter efficiently removes de noise without changing the peaks' shape. In this work Savitzky-Golay filter was applied using the MATLAB® function *sgolayfilt* to each retention time spectra. A 13 pixel window size and a 4th degree polynomial approximation was the configuration found empirically that produced the best results.

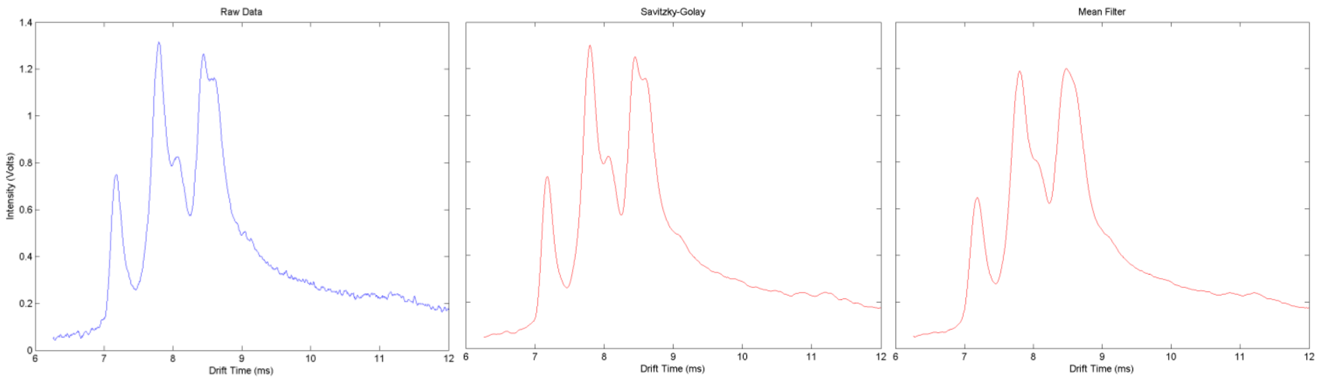

Figure 4.1 - Results of different filters applied in a single line spectrum

In figure 4.1 it can be clearly seen that the Savitzky-Golay filter reduces the noise in the data without changing the curve shapes like it happens in a moving average filter.

4.3.RIP Detailing

In order to facilitate the quantitative analysis of IMS the RIP tailing had to be described in a mathematical formula and then proceed to its removal. The IMS RIP has incremental contributions to the value of the peaks. To quantify the peaks, these contributions need to be found and removed. Based on the work of Bader et al. a lognormal equation was used to describe the RIP tail [**15**]. This lognormal equation in based on the lognormal statistical distribution. The calculation of the equation parameters required a series of steps as well as observation of the equation behavior in order to create reasonable bounds to those parameters.

The first step was to calculate the second derivative of the curve in order to find the major peaks. Then the Savitzky-Golay filter is applied to the second derivative result in order to facilitate the use of the *findpeaks* function of MATLAB®. The *findpeaks* function was sed to find the peaks that have at least 20% of the max value of the spectra and a minimum distance of 15 pixels between peaks. The position and the value of these peaks are then extracted to a data structure.

The second step uses the information saved in the data structure to create an estimation model. The number of peaks found decides the number of Inverse Gaussian Distribution curves it creates. The Inverse Gaussian distribution is an exponential

$$g_{\mu,\lambda}(x_i) = \sqrt{\frac{\lambda}{2\pi {x_i}^3}} \cdot \exp\left[-\frac{\lambda(x_i-\mu)^2}{2\mu^2(x_i)}\right], 0 < x_i < \infty \qquad 4.1$$

distribution with 2 parameters, μ and λ.

Where $\mu < 0$ is the mean and $\lambda < 0$ the shape. Its probability density function is given by the equation 4.1 and it's characterized by having a single peak and by not being symmetric, having a right tail. The position of the single peak is given by the mode. The mode depends on both parameters (μ, λ) and is given by $\left[\left(1+\frac{9\mu^2}{4\lambda^2}\right)^{\frac{1}{2}} - \frac{3\mu}{2\lambda}\right]$. For the modeling of a single curve two extra parameters were added. An intensity parameter that allows the curve to better adapt to the data and an offset x_0 that represents position where the curve starts.

The model consists in the major peaks, found with the second derivative and modeled with the Inverse Gaussian distribution curve, plus the lognormal function for the RIP tail. A function type file receives two structures, the drift time vector (tDrift) and a structure (GParameters) with all the parameters necessary to create the mathematical model.

The third step uses the Levenberg-Marquardt algorithm to find the ideal parameters for the model created. In order to apply the Levenberg-Marquardt algorithm we use the *lscurvefit* function of MATLAB®. This function receives the estimation model we want to use, a structure with the initial parameters, the values of the raw data, the tDrift, and two structures with the maximum and minimum bounds for the parameters.

The parameters bounds were added through the observation of the behavior of the curve. For the lognormal curve to best represent the RIP tail its behavior had to be controlled using a set of bounds within the Levenberg-Marquardt algorithm. These bounds are specific to the type of spectra used in this work. They ultimately limit the values found by the Levenberg-Marquardt algorithm, which means the values found may not be the most optional values in terms of the minimum value found by the error function but are the values that best represent the data.

Once the all parameters are found, they are introduced in the model function and the data representation is created. For the detailing of the RIP, only the parameters of the lognormal function are used.

The RIP detailing was tested in two different ways. In one the model fitting was applied to all the spectral lines and then the mean log normal curve was calculated. In the other way the mean spectrum was calculated and then the model fitting was applied to the mean spectrum.

The process where the fitting was applied to all the spectral lines produced good results but its time consumption was really high. The application of Levenberg-Marquardt algorithm in each line requires a really high processing power. Assuming that the model in average possesses 3 inverse Gaussian curves (4 parameters) and a lognormal curve (5 parameters), the algorithm had to calculate the optimal value of 17 parameters for each line. Even though this process produces more consistent results, the differences in results did not compensate the time spent. This process also had a different set of bounds of the lognormal curve then the other process, in table 4.1 the parameters used in this process is presented.

Table 4.1 - Initial parameters of lognormal curve and their upper and bottom bounds

	A	tDrift	μ	σ	b
First Estimation	0,01	6,2	1,3	1	0,1
Lower Bound	0	$\text{tDrift}_{\text{MIN}}$	0,5	0,5	0
Upper Bound	2	8	1,3	2	$\text{Intensity}_{\text{mean}}$

Calculating the mean spectrum along the retention time and then fit the model to this new data resulted in a faster process, mainly because the Levenberg-Marquardt algorithm runs a single time. In order for this method to work with acceptable results it required some customizations.

Table 4.2 - Initial parameters of lognormal curve and their upper and bottom bounds

	A	tDrift	μ	σ	b
First Estimation	0,01	6,2	1,3	1	0,1
Lower Bound	0	$\text{tDrift}_{\text{MIN}}$	0,5	0,5	0
Upper Bound	2	7,5	5	5	$\text{Intensity}_{\text{mean}}$

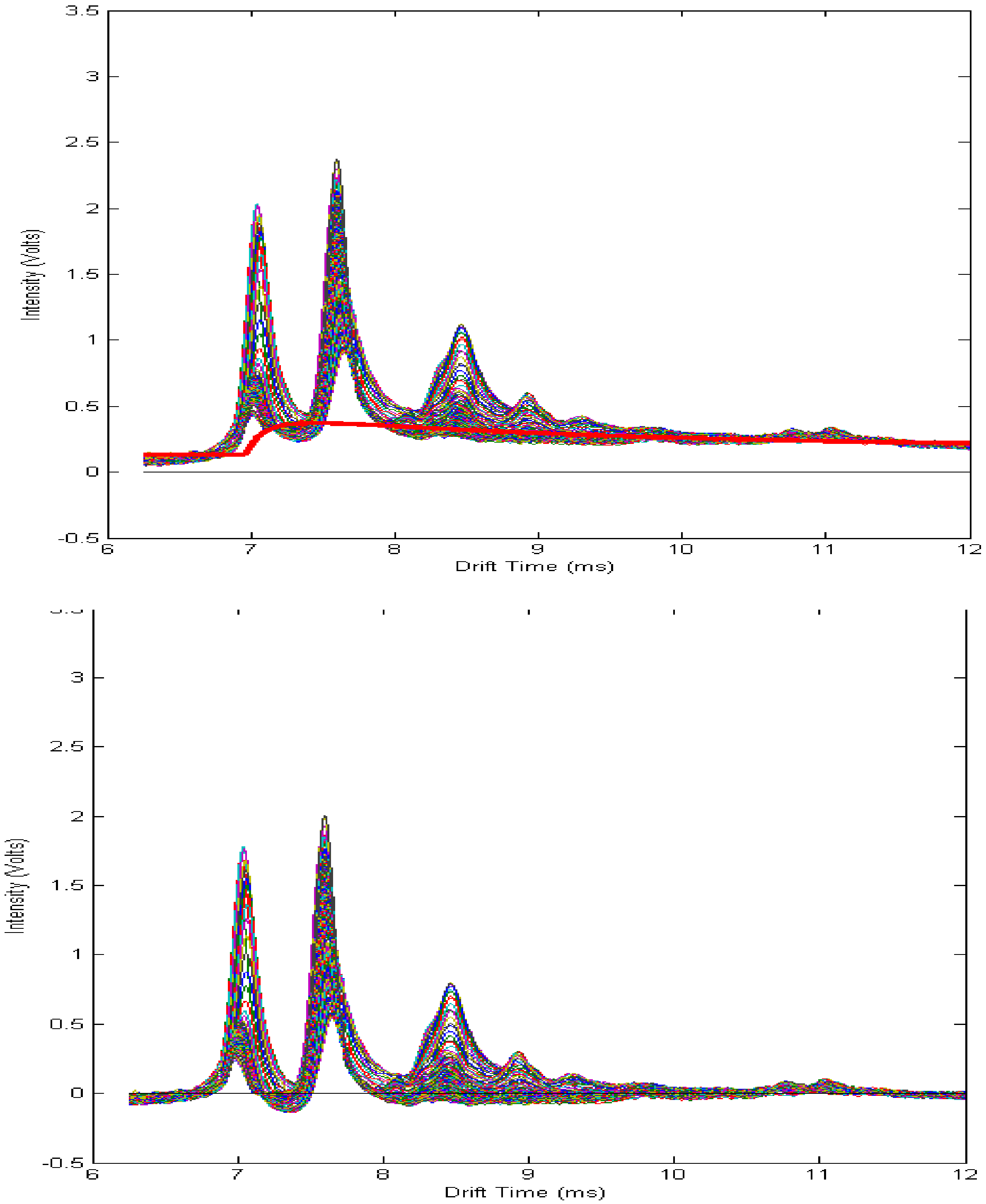

Figure 4.2 - Result of the rip detailling

The lognormal curve has a different set of bounds (table 4.2) and the process of finding peaks is wider in terms of the number of peaks it can find. This means that the model can find more curves, being more precise describing the mean spectrum. In figure 4.2 we can see an example of the RIP detailing. On the left is the result of the detailing and on the right is the plot of all the spectrum and the RIP tail curve that was calculated with the method developed.

4.4.Region of Interest

To find the correct position of the Acetone and Isoprene peaks it was necessary to find the region of interest in which the peaks were to be found using the spectral peak detection tool. This region of interest was found using several spectra that contained acetone and isoprene peaks.

Table 4.3 - Analysis of the empiric detection of acetone peak

	Acetone Peak	
	tDrift (ms)	tRet (s)
Average	8,543	8,737
Standard Deviation	0,056	0,908
Maximum Values	8,653	9,828
Minimum Values	8,440	6,174

In table 4.3 and 4.4 the positions of the acetone and isoprene peaks extracted empirically are presented. It can be seen that the position of the acetone peak is very contained in the tDrift axis, with its average value being 8,543ms and with a standard deviation of 0,056ms, indicating that the value does not deviates much from its average value. On the other hand the position on the tRet axis has a wider range with the average value being at 8,737s with a standard deviation of 0,908s. This wider range is justified by some peaks reaching a maximum of 9,828s (~+1) and a minimum of 6,174s (~+2), indicating some considerable fluctuation in the tRet.

Table 4.4 - Analysis of the empiric detection of isoprene peak

	Isoprene Peak	
	tDrift (ms)	tRet (s)
Mean	8,384	8,285
Standard Deviation	0,053	0,878
Maximum Values	8,568	9,324
Minimum Values	8,286	5,922

Isoprene peak position has an average tDrift value of 8,384ms with a standard deviation of 0,053ms and an average tRet value of 8,285s with a standard deviation 0,878s. Once again there are some fluctuations in the tRet axis which affect the uncertainty of the isoprene peak. The standard deviation of both peaks is similar, which assures that the peak positioning is consistent despite being different substances.

Table 4.5 - Analysis of the empiric region of interest

	Region			
	Average	Standard Deviation	Maximum	Minimum
Bottom tDrift (ms)	8,22961	0,05651	8,38600	8,14000
Top tDrift (ms)	8,75627	0,07078	8,98000	8,58600
Bottom tRet (ms)	6,90348	0,69106	8,06400	5,16600
Top tRet (ms)	11,77109	1,35701	16,51000	9,07200
Surface (ms^2)	2,59745	0,84202	6,55829	1,60149
Dif tDrift (ms)	0,52666	0,05738	0,75400	0,39300
Dif tRet (ms)	4,86761	1,10720	9,07600	2,89600

Table 4.5 gives the information of the region that contains the peaks. The region contains the relevant area to correctly quantify the peaks. Once more the range in the tDrift axis does not vary much, which correlates to the fact that the Drift time is related to the ionic mobility of the substances. Using this information the region of interest was defined as μ+2σ to the top values of tDrift and tRet and as μ-2σ to the bottom values of tDrift and tRet. This resulted in a region with a top corner situated at (8,8978ms ; 14,4851s) and a bottom corner situated at (8,1166ms ; 5,5214s).

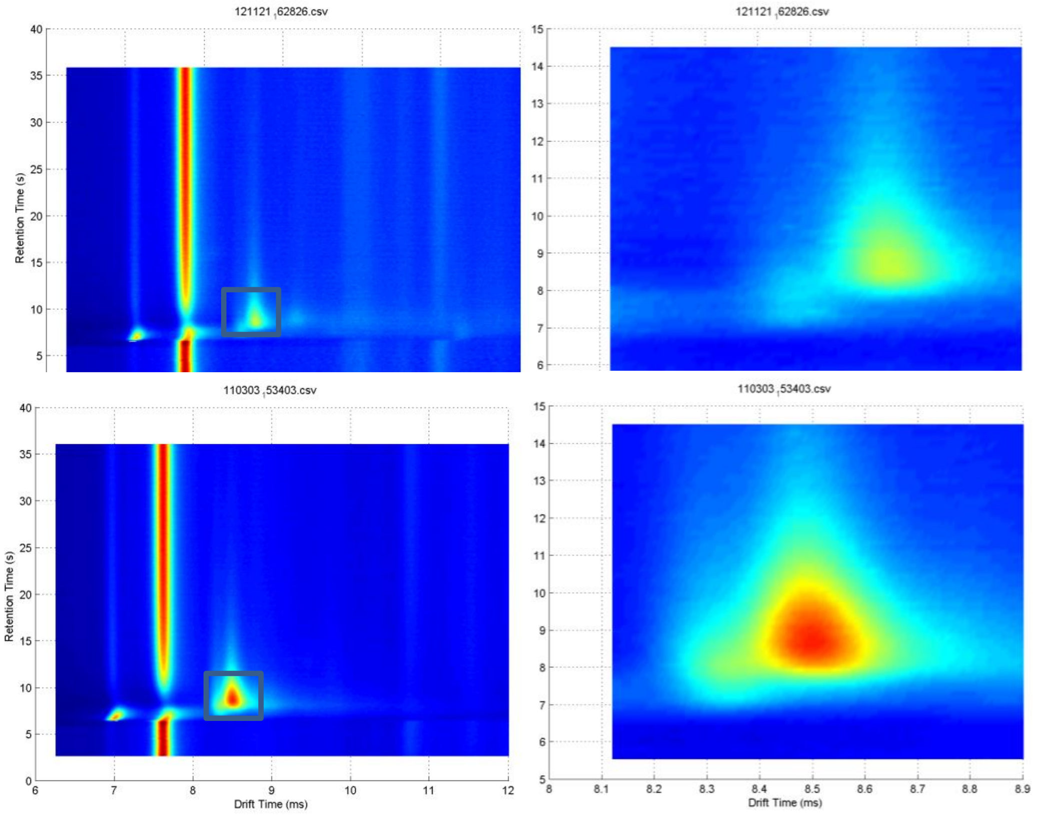

FIGURE 4.3 - Example of the region of interest selection

In figure 9 we have two examples of the region of interest implemented in the algorithm. The region chosen has the necessary information for the peak detection and fitting.

4.5.Spectral peak detection

For the spectral peak detection the gradient path labeling algorithm (GPL) was used [**20**]. GPL detects the regional maximums in the region of interest chosen earlier. Because a gradient image have a confluence of several ascending paths towards a regional maximum, GPL is a method of segmentation based on the labeling of these gradient paths. The algorithm is divided in two stages.

The first stage starts by attributing a label to each pixel of the image in a top-left to bottom-right direction and determining its gradient azimuth using a 3x3 *Sobel* operator. Once all the pixels are labeled the algorithm propagates the labels following the gradient path until an already marked or outside image boundaries pixel is found. When the propagation finishes on a different label, the two labels are tagged as *equivalents* and considered to belong to the same maximum.

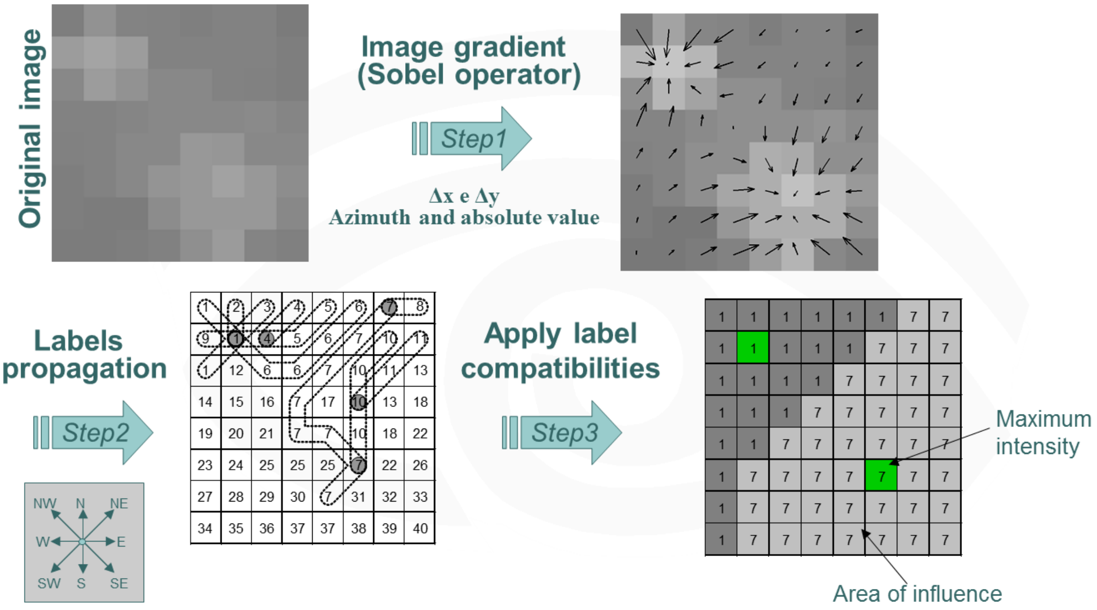

1	2	3	4	5	6	7	8
9	1	4	5	6	7	10	11
1	12	6	6	7	10	11	13
14	15	16	7	17	10	13	18
19	20	21	7	7	10	18	22
23	24	25	25	25	7	22	26
27	28	29	30	7	31	32	33
34	35	36	37	37	38	39	40

1	1	1	1	1	1	7	7
1	1	1	1	1	7	7	7
1	1	1	1	7	7	7	7
1	1	1	7	7	7	7	7
1	1	7	7	7	7	7	7
1	7	7	7	7	7	7	7
1	7	7	7	7	7	7	7
1	7	7	7	7	7	7	7

Figure 4.4 - Peak detection algorithm example

The second stage of the algorithm is when the *equivalences* are applied and the image is segmented and each segment is a maximum or, in the context of this work, is a peak.

Due the shape of the curves, not all gradient paths end on the same maximum pixel, resulting in over-segmentation of the image. Although a merging method exists in the GPL algorithm, it was not sensitive enough to correctly detect the peaks. In order to extract the correct position of the isoprene and acetone peaks, the regional maximums detected by the GPL are posteriorly filtered. The filter applied has 3 steps and is based in the empiric observation of various spectra presented in the region of interest chapter (5.4). First the method checks if any peaks are present in an area with one standard deviation of uncertainty around the average value of the peaks. If no peaks are found the method passes to the second step, this one is basically equal to the first but widens up the area to two standard deviations on uncertainty. If more than one peak is found, the method picks the one with the highest intensity.

4.6.Spectral peaks modeling

The substance peaks in the IMS spectra, at first sight, look like they can be described by a Gaussian curve, but the elongations in tDrift and tRet discredit the first observation. Based on the work of Kopcynski, Baumbach, and Rahmann and the observation of various spectra the Inverse Gaussian Distribution curve was found to be the equation that could be used to describe the peaks with the elongations [**19**].

$$\mathrm{f(x,y)} = \begin{cases} 0 & \mathrm{x < x_0 \text{ or } y < y_0} \\ A \cdot \sqrt{\dfrac{\lambda_x}{2\pi(\,x - x_0)^3}} \cdot exp\left[-\dfrac{\lambda_x\big((x - x_0) - \mu_x\big)^2}{2{\mu_x}^2(x - x_0)}\right] \cdot \sqrt{\dfrac{\lambda_y}{2\pi(\,y - y_0)^3}} \cdot exp\left[-\dfrac{\lambda_y\Big((y - y_0) - \mu_y\Big)^2}{2{\mu_y}^2(y - y_0)}\right] & else \end{cases}$$

To develop the 3D model that describes the IMS peaks, two Inverse Gaussian Distribution curves were multiplied, one representing the tRet axis and another the tDrift axis. The curves also had some changes to the original equation in order to be able to adapt to the IMS data. These changes consisted in adding two new parameters, the intensity (A_x,A_y) and the position of the beginning of the curves (x_0, y_0). In the final model a single parameter for the intensity (A) appears due to the multiplication of A_x and A_y, the reduction of the parameters number simplifies and reduces the number of calculations needed to find the optimal value.

During the peak location stage, the algorithm finds the position of the peaks however the model uses the position of the start of the curve making it necessary the calculation of the position of the peak related to the start of the curve. This is achieved using the mode of each curve. The mode gives the position of the maximum value relatively to the start of the curve. Using this information the position of the peak in tRet and tDrift is given by $x_0 + mode_x$ and $y_0 + mode_y$.

The Levenberg-Marquardt algorithm is used to find the parameters that allow the model to best adapt to the data, resorting once again in the MATLAB® *lscurvefit* function. The *lscurvefit* function receives the region of interest data, a structure containing both the tDrift and tRet vectors of the region of interest in grid form, a structure with all the initial parameters to the model, and two structures with the top and low bounds for the parameters.

The tDrift and tRet vector were transformed into matrices using the *meshgrid* function of MATLAB®, this step was a necessity due to the characteristics of *lscurvefit*, because as the name implies it's a function for curves and not surfaces, this was circumvented using a single structure with both vectors as grids. The other reason this method works is because once the data enters the function, the Levenberg-Marquardt algorithm does not care it it's a curve or a surface and resolves the non-linear problem presented.

The initial parameters are generic values for the peak shape and the positions detected by the GPL for the peak location. The Levenberg-Marquardt algorithm receives the parameters for the number of peaks detected plus one additional peak. This additional peak helps the algorithm to shape the model to the best fit possible, it also tries to stop the algorithm to try to compensate noise structures with the peaks.

The parameters bounds were chosen based on the observation and testing of the Levenberg-Marquardt algorithm in a series of spectra. These bounds give enough freedom to the algorithm without de-characterizing the curves, in order to get the best fit possible.

Table 4.6 - Initial parameters and their upper and lower bounds for the peaks model

	A	tDrift			tRet		
		x_0	λ	μ	y_0	λ	μ
Estimation	GPL	GPL	1	1	GPL	1	1
Lower Bound	0	GPL - 0,05	0,5	0,1	GPL - 0,9	0,5	0,1
Upper Bound	10	GPL + 0,05	100	10	GPL + 0,9	100	10

With the parameters found, seven for each peak, a recreation of the data is produced that can be used for comparison with the data. To evaluate the goodness of the fit it is possible to calculate the total volume of both images and compare the values. It is also possible to calculate the mean squared error between each pixel of the image.

The parameters found can be used to compute each peak individually. This representation is used to quantify both isoprene and acetone. This quantification is an absolute value that can be later used to create a relation with volume values of these substances.

5. Results of Peak Analysis

For data analysis there are two main indicators being evaluated, the automatic detection of the peaks and the goodness of the fit. These two indicators are the ones that best assess the quality of the algorithm. Good automatic peak detection is essential for future works and has multiple applications. The goodness of the fit can be used to validate if the chosen method and model are correct to quantify substances in MCC-IMS spectra.

5.1.Peak Detection

To give an overview of the results produced by the GPL algorithm the same spectra empirically analyzed were analyzed by the algorithm and a comparison of the results is presented here. A total of 77 spectra with isoprene and acetone peaks were analyzed. The average value of the peaks and its respective standard deviation will be analyzed as well as the differences in the position of the peaks in each spectrum.

5.1.1. Acetone Peak

In the spectra analyzed the acetone peak is usually the most intense. As it was referred before, it is located around the point (8,543ms; 8,737s). In table 5.1 is given an overview of the differences between the empiric detection and the automated detection. The differences in value of the mean value and the standard deviation are small, what may indicate a good behavior of the algorithm, although not enough to formulate a conclusion.

Table 5.1 - Results of the acetone peak detection

	Acetone Peak					
	Empiric		*GPL*		*Difference*	
	tDrift (ms)	*tRet (s)*	*tDrift (ms)*	*tRet (s)*	*tDrift (ms)*	*tRet (s)*
Mean	*8,54261*	*8,73677*	*8,51618*	*8,59091*	*0,02643*	*0,14586*
Standard Deviation	*0,05637*	*0,90752*	*0,04620*	*0,87877*	*0,01017*	*0,02874*

In order to get a better overview of the GPL algorithm's behavior, in figure 5.1 the multiple acetone peaks detected, empirically and by the algorithm, are presented. Here it's displayed the position of the mean value for each detection method, with error bars representing two standard deviation of uncertainty. It can be noticed that the peak positions follow a similar distribution. The average error between peaks detected by both methods is 0,50% in the tDrif axis and 6,89% in the tRet axis, although in some cases in the tRet axis the error is up to 60,78%. According to these values, it can ve concluded that the acetone peak is being correctly detected by the algorithm.

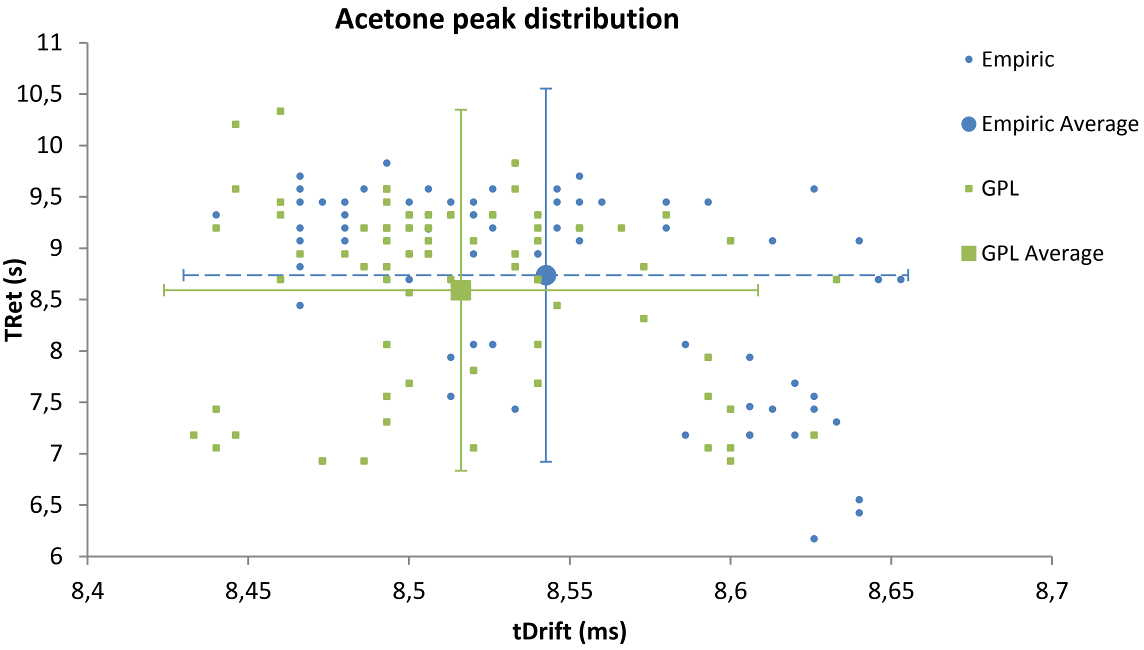

Figure 5.1 - Acetone peaks distribution

5.1.2. Isoprene Peak

In the analyzed spectra the isoprene peak is not always present and is usually less intense than the acetone peak.

Table 5.2 - Results of the isoprene peak detection

	Isoprene Peak					
	Empiric		GPL		Difference	
	tDrift (ms)	tRet (s)	tDrift (ms)	tRet (s)	tDrift (ms)	tRet (s)
Mean	8,38416	8,28520	8,37467	7,73951	0,00949	0,64465
Standard Deviation	0,05248	0,87764	0,05918	0,98086	0,00670	0,10322

In table 5.2 it can be seen that the differences in the tDrift values are minimal and in the tRet, although bigger than the differences in tDrift, are small enough to get a good overview in the quality of the detection.

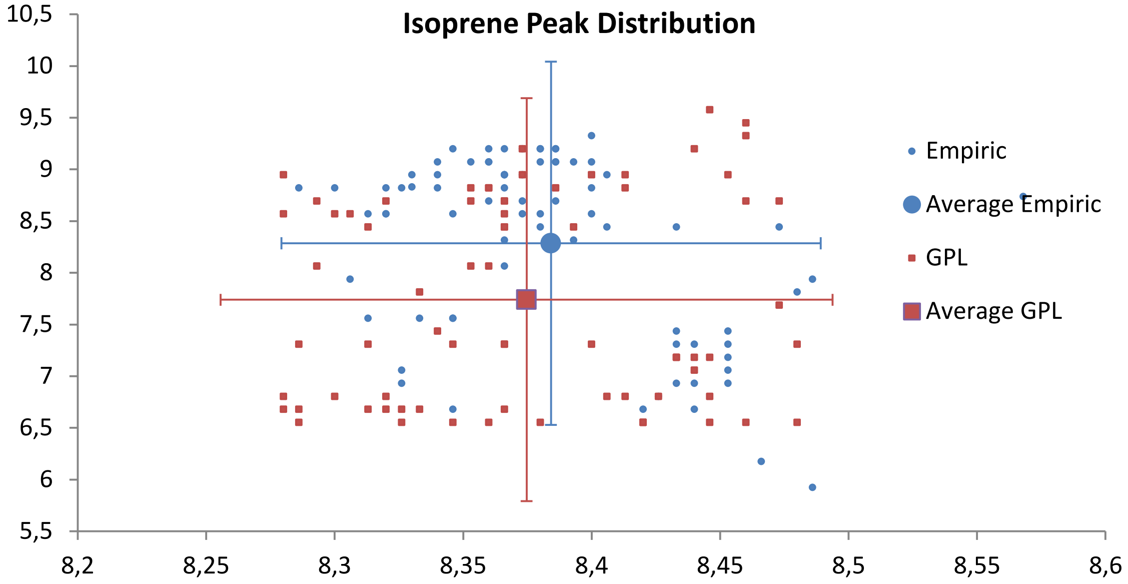

Figure 5.2 - Isoprene peaks distribution

In figure 11 the distribution of the peaks is represented, once again with the position average value and its respective error bars with a two standard deviation uncertainty. The behavior of the algorithm when detecting the isoprene peak is also very good. With an average error of 0,48% in the tDrift axis and 8,67% in the tRet axis, and a maximum error of 2,43% in the tDrift axis and 44,68% in the tRet axis. It can be concluded that the algorithm detects the correct position of the isoprene peak. It is also worth to mention that some isoprene peaks were not detected by the algorithm. There are two reasons for this. In some spectra the acetone peak was so intense that masked the isoprene peak. While in other spectra the isoprene peak was so small that the algorithm ignored it because it didn’t have enough intensity.

5.2.Fit

To have a perception of the goodness of the fit first the analysis will focus in a single spectrum and then a statistical overview of a series of tests will be presented.

This spectrum went through the whole process algorithm and the results are going to be discussed.

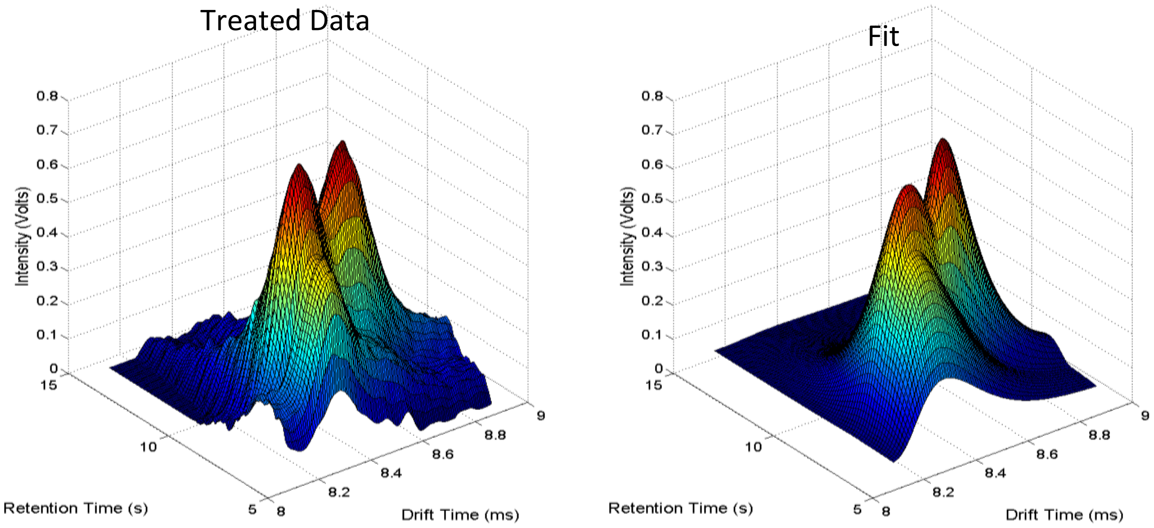

Figure 5.3 - Result of the fit

Figure 5.3 is presents the result of the fit. It can be observed the presence of 3 peaks. At first sight the main difference is how smooth the fit is. In the treated data the position of the acetone peak, found by the detection method, was 8,500ms in tDrift and 7,938s in tRet and in the fit its position is 8,493ms in tDrift and 9,938s in tRet. As for the isoprene peak the detection method determined its position was 8,313ms in tDrift and 7,308s in tRet and in the fit its position was 8,340ms in tDrift and 7,560s in tRet, we can conclude that the peaks position is correct, as was expected. A third peak was also added in order to get the best fit possible.

Having the fit similar to the data is not enough. To have a perception of the fit result the absolute volume of both matrices was calculated. To find the volume beneath each surface the discrete integral of both surfaces was calculated. Because both surfaces are matrices of the same size the computation of the discrete integral becomes trivial. Assuming the surface is divided in the same number of unitary divisions, the contribution to volume is only the intensity. So summing all the intensities in the image we have the volume beneath the surface. The absolute volume of the treated data was 1365,44 and the volume of the fit was 1459,09. This means a difference in volumes of 6,86% with a mean squared error between each pixel of the images of 0,002.

Table 5.3 - Parameters of the each individual peak

Peak	A	tDrift			tRet		
		x_0	λ	μ	y_0	λ	μ
Acetone	0,2350	8,5142	0,5125	0,2569	8,0084	12,4926	2,2546
Isoprene	0,5356	8,3152	2,0120	0,3664	7,0080	63,5250	8,9232
Additional	0,1473	8,3565	9,6718	0,5011	7,7328	3,2109	2,2416

Table 5.3 contains the parameters found by the Levenberg-Marquardt algorithm these parameters are used to represent the acetone and the isoprene peak individually. Using these parameters it’s possible to calculate the absolute volume of each individual peak.

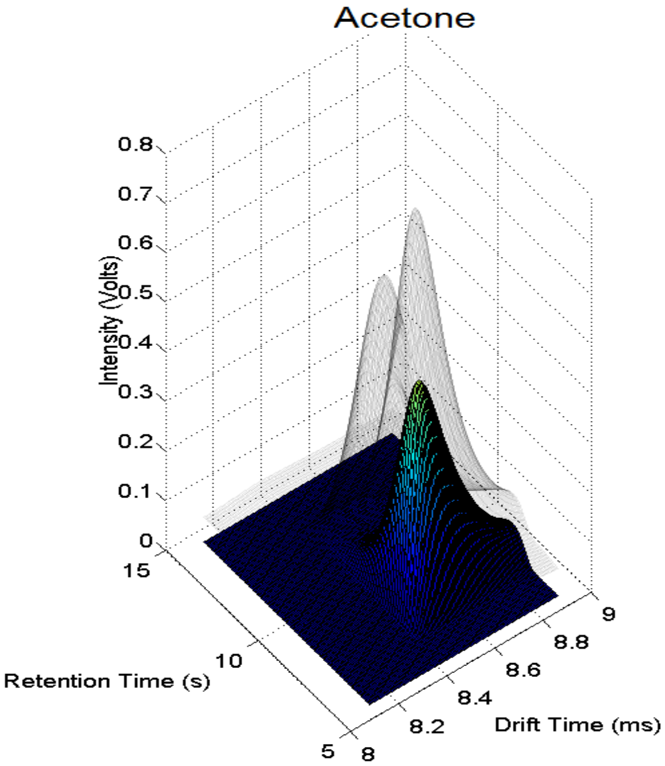

Figure 5.4 - Acetone peak isolated

In figure 5.4 and figure 5.5 we have the acetone and isoprene peaks, respectively. It is possible to observe how each peak contributes to the fit result.

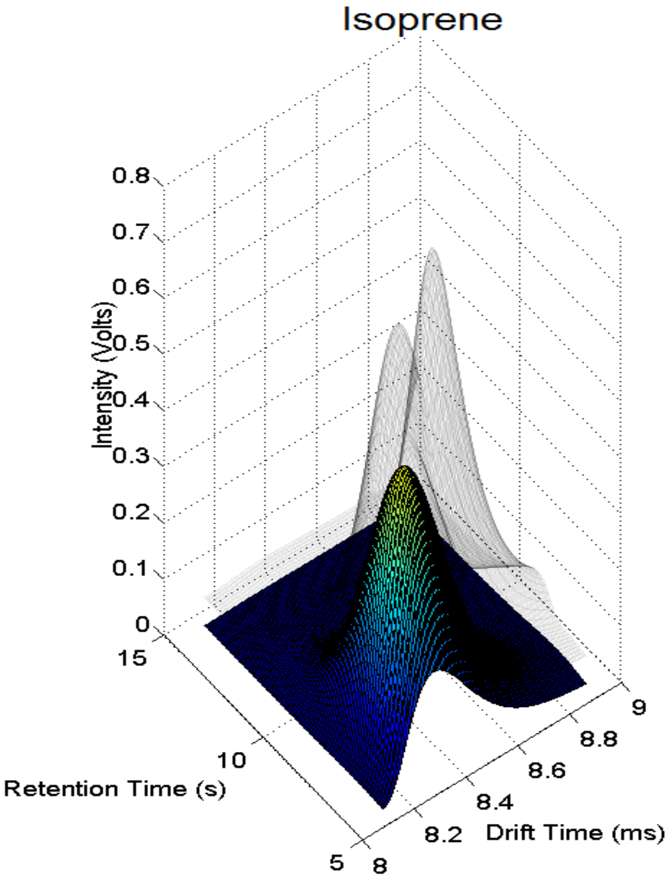

Figure 5.6 - Isoprene peak isolated

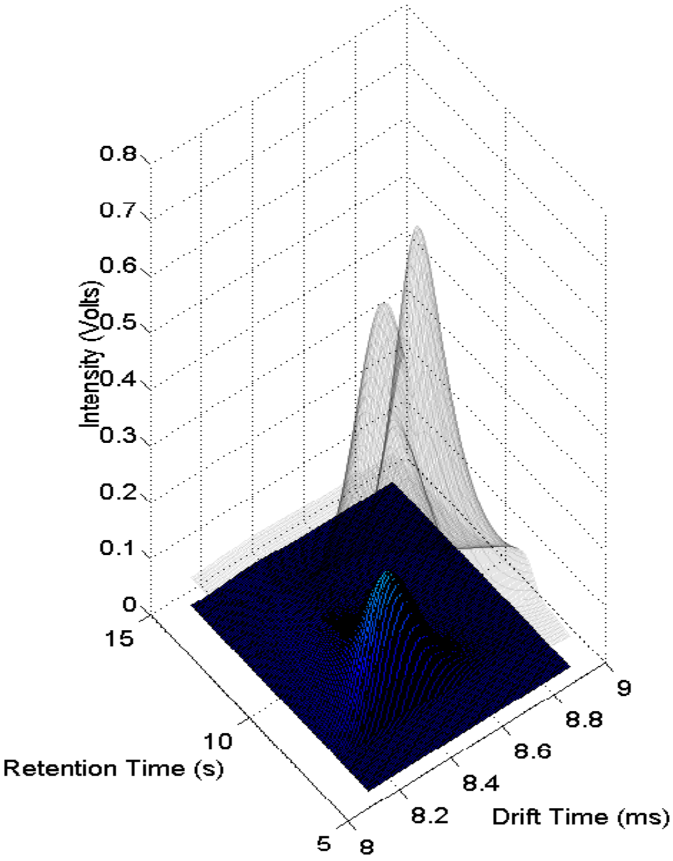

Figure 5.5 - Third peak isolated

The value of the absolute volume of each peak was 256,33 for acetone, 606,42 for isoprene, and 171,539 for the third peak. Although the results of the algorithm show that the isoprene has a higher volume then the other peaks, no conclusions can be made in terms of what substance has higher concentration in the analyzed sample.

5.3.Peak Volumes

To have an overall review of the fitting process several spectra were analyzed. The algorithm returned for each spectrum an image of the data and an image of the fit and a text file with the values of the volumes and the mean squared error calculated.

Due to the nature of the Levenberg-Marquardt algorithm, not all the fitting were satisfactory, as some fits could not characterize correctly all the peaks. The algorithm was able to produce good fits in 59,2% of the cases and the average difference between the volume of the data and the fit was 11,37%. Separating the good fits from the bad fits, we have a difference in volume of 10,4% for the good fits and a difference of 12,8% for the bad fits.

In terms of the mean squared error between the data and the fit the average value was 0,00295. Once again separating the good fits from the bad fits produced a different result. For the good fits the average value of the mean squared error was 0,00158 and for the bad fits was 0,00494.

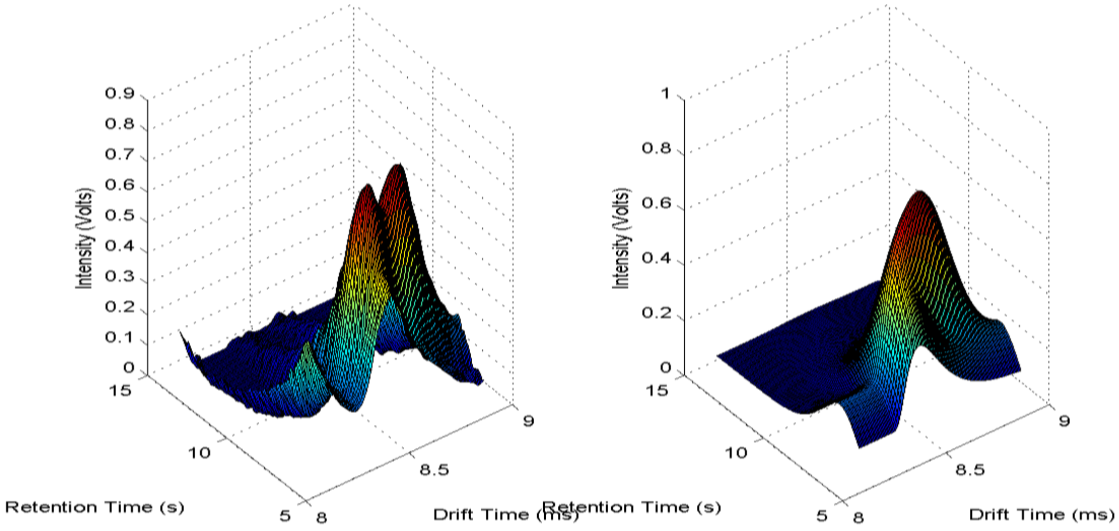

Figure 5.7 - Example of a bad fit

Analyzing the results it can be concluded that a good fit is less associated with the volume difference and more associated with differences at pixel level. Also some of the bad fits, result from spectra that possess acetone and isoprene peaks that are too close (Figure 5.7), leading the Levenberg-Marquardt algorithm to represent the two peaks as just one, leading to a poor fit.

6. Concluding Remarks

This thesis is the result of the creation of a methodology to automatically identify and quantify isoprene and acetone peaks, using to image processing techniques. The sequence of methods applied to the raw data was the result of a series of developments and tests in order to achieve the proposed objective, to identify and quantify isoprene and acetone peaks in MCC-IMS spectra.

Generally speaking the objective of the proposed work was achieved: the algorithm was able to identify and quantify isoprene and acetone.

The analysis shows that the algorithm was able to effectively treat the data by correctly attenuating the noise, removing the RIP tail, detecting and identifying isoprene and acetone peaks, and finally fitting de data to the custom model.

We can conclude that de chosen mathematical models to describe the RIP tail and to describe the peaks produce convincing results and that with some fine tuning can offer even better results.

In terms of isoprene and acetone detection and identification it's possible to conclude that the algorithm reliably detects and identifies the correct position of the peaks with minimal deviations.

In the quantification the produced results were not as positive. The Levenberg-Marquardt algorithm doesn't always produce the best result, creating fits that don't represent the data in a reliable way but only when the two peaks are present are overlapped. If a single peak is present the algorithm offers a good result in terms of quantification.

The solution to the problem relies in finding better parameter bounds to the peaks, finding a better way to eliminate the RIP tail, and find a curve to better represent the peaks base. These solutions all require further testing with specific spectra that produce expected results in order to tune the parameters of the curves and their respective values.

The algorithm developed in this work achieved promising results in terms of detecting and quantifying the isoprene and acetone peaks in MCC-IMS spectra. These results were exposed in the *8th International Conference on Breath Research & Cancer Diagnosis* and received a recommendation for the creation of a scientific paper.

6.1. Future Work

The developed algorithm has plenty of future works. To have better parameter boundaries it is proposed to test samples of known concentrations of isoprene and acetone. The spectra produced with these tests will have characteristic shapes and behaviors depending on the concentrations used, for example it can be determined the shape of a single acetone peak without isoprene present, it can also be determined the behavior of the overlapping peaks depending in what substance has a higher concentration in the testes sample.

These tests will also provide means for the creation of calibration curves between the volume calculated by the algorithm and the concentration of substances.

Finally for further research it is also proposed to proceed the testing with different substances. These different substances produce different peaks in different positions, requiring a more complex algorithm to detect the various VOCs present in a MCC-IMS spectrum. Looking at the future the ideal algorithm is one that receives a spectrum and identifies all the meaningful substances and their respective concentration.

Bibliography

[1] William F. Siems, and Robert H. St. Louis Herbert H. Hill Jr., "Ion Mobility Spectrometry," *Analytical Chemistry*, no. 62, pp. 1201A - 1209A, 1990.

[2] Gary A. Eiceman Jorg Ingo Baumbach, "Ion Mobility Spectrometry: Arriving On Site and Moving Beyond a Low Profile," *Applied Spectroscopy*, vol. 53, no. 9, pp. 338A-355A, 1999.

[3] G.A.S., Gas Chromatograph-Ion Mobility Spectrometer, Technical Documentation.

[4] Toshiaki Funada and Takao Tsuda Tetsuo Ohkuwa, "Acetone Response with Exercise Intensity," in *Advanced Gas Chromatography - Progress in Agricultural, Biomedical and Industrial Applications*, Dr. Mustafa Ali Mohd, Ed., 2012, ch. 8, pp. 151-160.

[5] Miklós Péter Kalapos, "On the mammalian acetone metabolism: from chemistry to clinical implications," *Biochimica et Biophysica Acta* , no. 1621, pp. 122-139, 2003.

[6] Rossana Salerno-Kennedy and Kevin D. Cashman, "Potential applications of breath isoprene as a biomarker in modern medicine: a concise overview," *The Middle European Journal of Medicine*, pp. 180-186, 2005.

[7] Jochen K. Schubert, Gabriele F.E. Noeldge-Schomburg Wolfram Miekisch, "Diagnostic potential of breath analysis—focus on volatile organic compounds," *Clinica Chimica Acta*, no. 347, pp. 25-39, 2004.

[8] Peter Prazeller, Dagmar Mayr, Alfons Jordan, Josef Rieder, Ray Fall, Werner Lindinger Thomas Karl, "Human breath isoprene and its relation to blood cholesterol levels: new measurements and modeling," *Journal of Applied Physiology*, no. 91, pp. 762-770, Aug 2001.

[9] Jorg I. Baumbach, Wolfgang Vautz Chandrasekhara B. Hariharan, "Linearized Equations for the Reduced Ion Mobilities of Polar Aliphatic Organic Compounds," *Anal. Chem.*, no. 82, pp. 427-431, 2010.

[10] J.I. Baumbach J. Stach, "Ion Mobility Spectrometry - Basic Elements and Applications," International Society for Ion Mobility Spectrometry, 2002.

[11] "Vera Ruzsanyi, Jorg Ingo Baumbach, Stefanie Sielemann, P. Litterst,M. Westhoff, Lutz Freitag," *Journal of Chromatography A*, no. 1084, pp. 145–151, 2005.

[12] Marcel J. E. Golay Abraham Savitzky, "Smoothing and Differentiation of Data by Simplified Least Squares Procedures.," *Analytical Chemistry*, no. 36, pp. 1627-1639, 1964.

[13] R. W. Schafer, ""What is a Savitzky-Golay filter"," *IEEE Signal Processing Magazine*, vol. 28, no. 4, pp. 111-117, 2011.

[14] Fredrik Jonsson. (2011) SGFilter - A stand-alone implementation of the Savitzky–Golay

smoothing filter.

[15] Sabine Bader, "Identification and Quantification of Peaks in Spectrometric Data," Technical University of Dortmund, Dortmund, 2008.

[16] Alexander Bunkowski, "MCC-IMS data analysis using automated spectra processing and explorative visualization methods," University Bielefeld, Bielefeld, 2011.

[17] W.S. Cleveland, "Robust locally weighted regression and smoothing scatterplots," *J. Am. Stat. Assoc.*, no. 74, pp. 829–836, 1979.

[18] Y. Yasui T.W. Randolph, "Multiscale processing of mass spectrometry data," *Biometrics*, no. 62, pp. 589-597, 2006.

[19] Jorg Ingo Baumbach, Sven Rahmann Dominik Kopczynski, "Peak modeling for ion mobility spectrometry measurements," in *20th European Signal Processing Conference*, Bucharest, 2012.

[20] André D. Mora, Pedro M. Vieira, Ayyakkannu Manivannan, and José M. Fonseca, "Automated drusen detection in retinal images using analytical modelling algorithms," *BioMedical Engineering OnLine*, no. 10, January 2011, doi:10.1186/1475-925X-10-59.

[21] urgen Nolte, Rita Fobbe and org Ingo Baumbach Wolfgang Vautz, "Breath analysis—performance and potential of ion mobility spectrometry," *Journal of Breath Research*, no. 3, 2009.

[22] Wilson HK, "Breath Analysis. Physiological basis and sampling techniques.," *Scand J Work Environ Health 12*, pp. 174-192, 1986.

[23] R. Fuoco, M.G. Trivella, A. Ceccarini F. Di Francesco, "Breath analysis: trends in techniques and clinical applications," *Microchemical Journal 79*, pp. 405-410, 2005.

[24] Till Schneider, Josch Pauling, Kathrin Rupp, Mi Jang, Jörg Ingo Baumbach and Jan Baumbach Anne-Christin Hauschild, "Metabolomic Data Analysis of Ion Mobility Spectrometry Data - Reviewing the State of the Art," *Metabolites*, no. 2, pp. 733-755, 2012.

[25] Magdalena Ligor, Anton Amann, Boguslaw Buszewski Agnieszka Ulanowska, "Determination of Volatile Organic Compounds," *Chem. Anal. (Warsaw)*, no. 53, 2008.

Appendix A

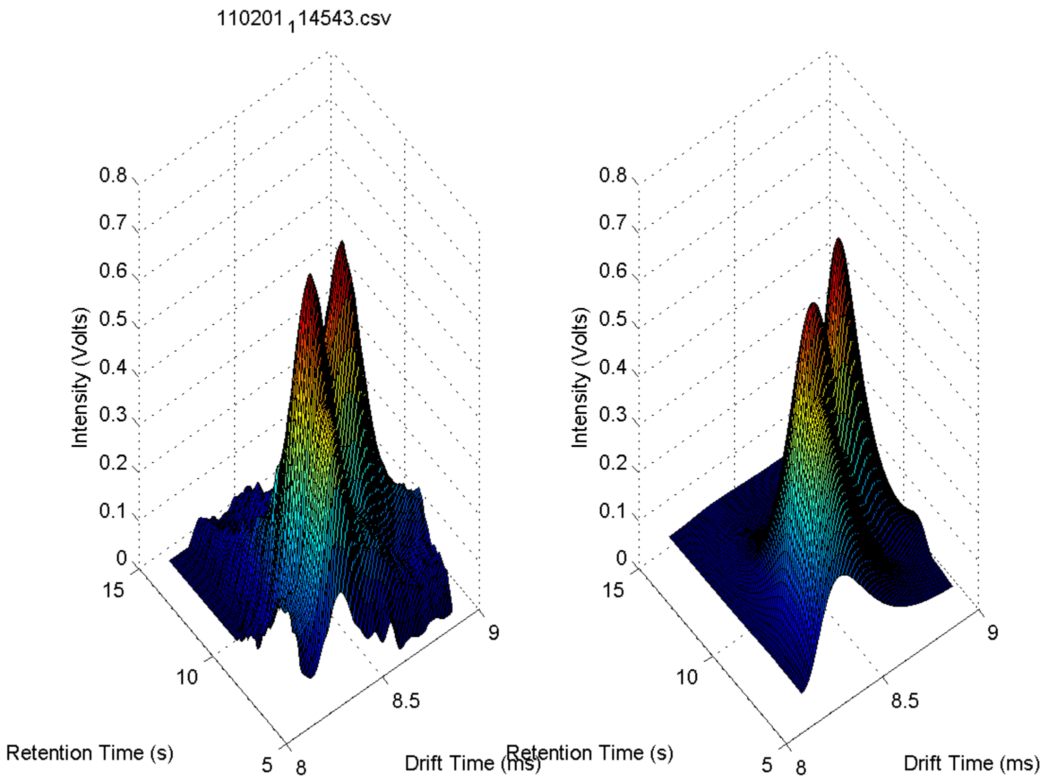
110201 $_1$14543.csv
Intensity (Volts)
0.8
0.7
0.6
0.5
0.4
0.3
0.2
0.1
0
15
10
5
Retention Time (s)
8
8.5
9
Drift Time (ms)
Intensity (Volts)
0.8
0.7
0.6
0.5
0.4
0.3
0.2
0.1
0
15
10
5
Retention Time (s)
8
8.5
9
Drift Time (ms)

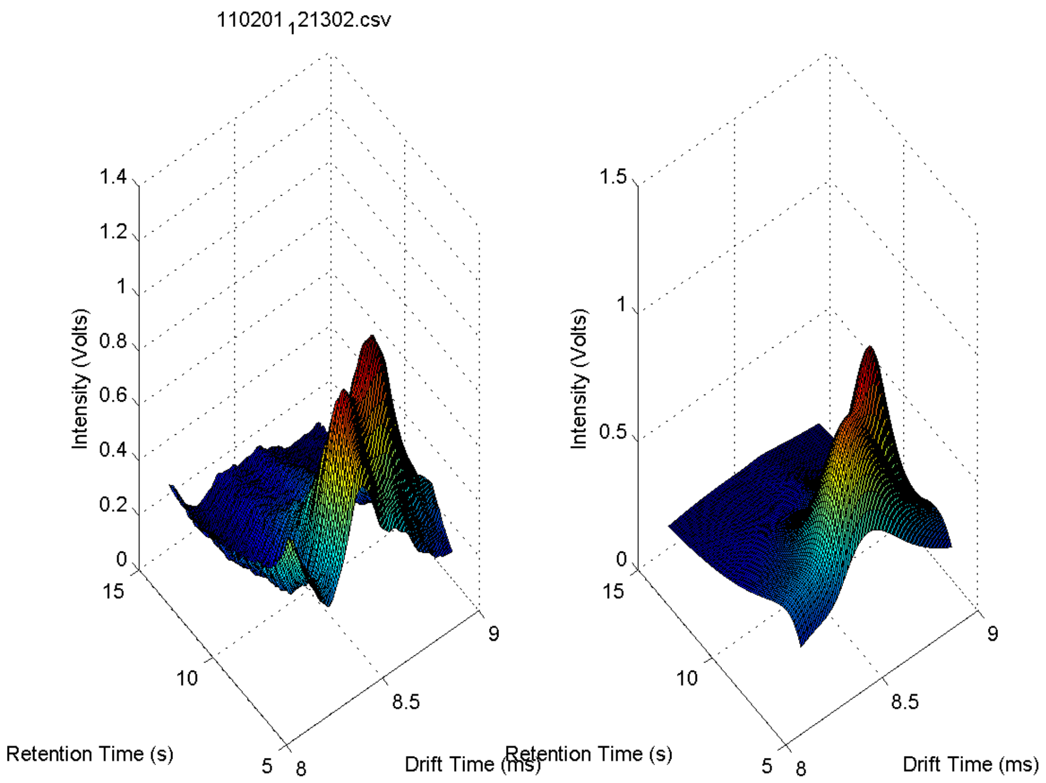
110201 $_1$21302.csv
Intensity (Volts)
1.4
1.2
1
0.8
0.6
0.4
0.2
0
15
10
5
Retention Time (s)
8
8.5
9
Drift Time (ms)
Intensity (Volts)
1.5
1
0.5
0
15
10
5
Retention Time (s)
8
8.5
9
Drift Time (ms)

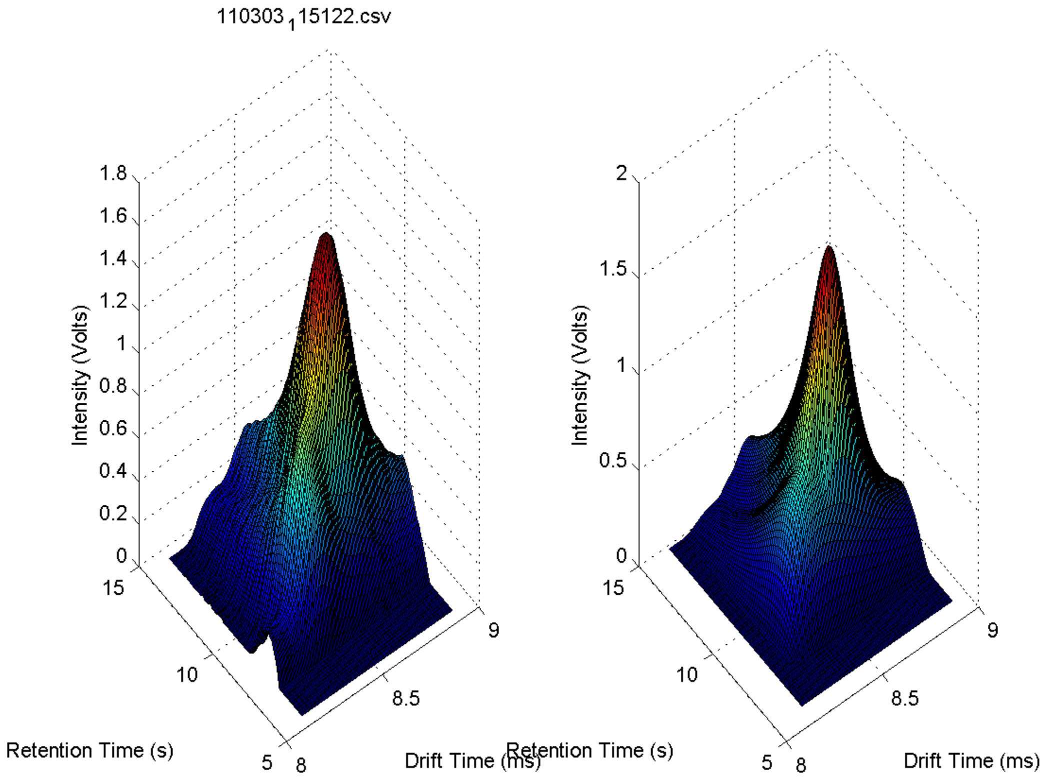
110303$_1$15122.csv
Intensity (Volts)
0
0.2
0.4
0.6
0.8
1
1.2
1.4
1.6
1.8
15
10
5
Retention Time (s)
8
8.5
9
Drift Time (ms)
Intensity (Volts)
0
0.5
1
1.5
2
15
10
5
Retention Time (s)
8
8.5
9
Drift Time (ms)

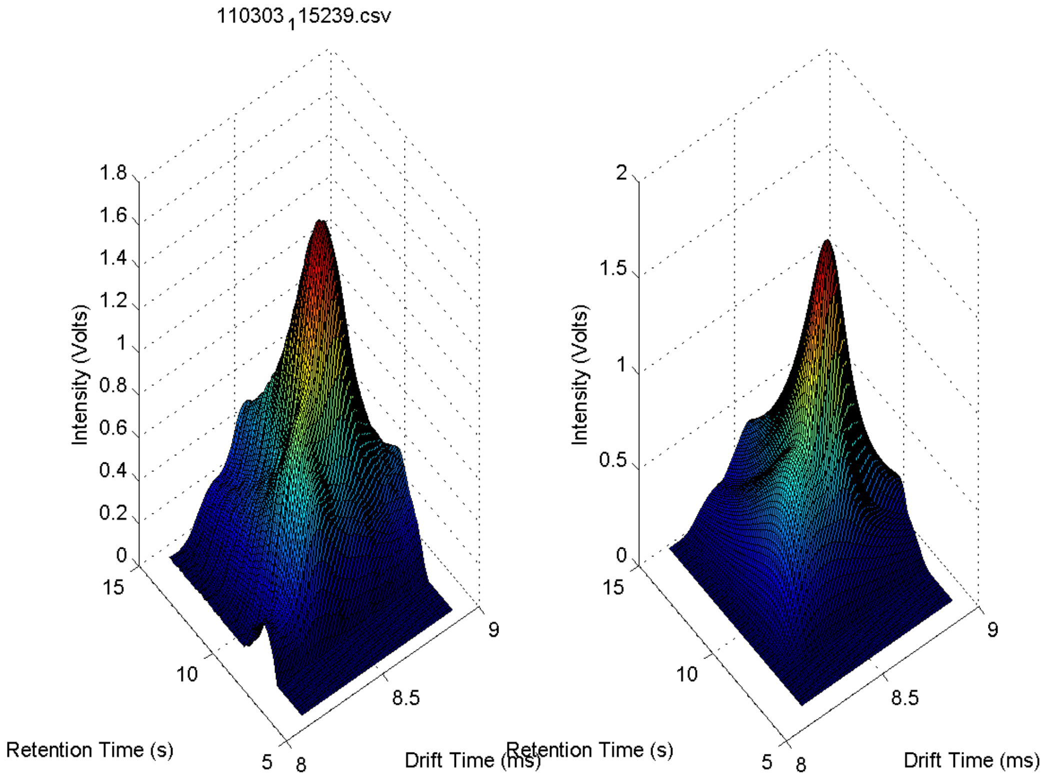
110303$_1$15239.csv
Intensity (Volts)
0
0.2
0.4
0.6
0.8
1
1.2
1.4
1.6
1.8
15
10
5
Retention Time (s)
8
8.5
9
Drift Time (ms)
Intensity (Volts)
0
0.5
1
1.5
2
15
10
5
Retention Time (s)
8
8.5
9
Drift Time (ms)

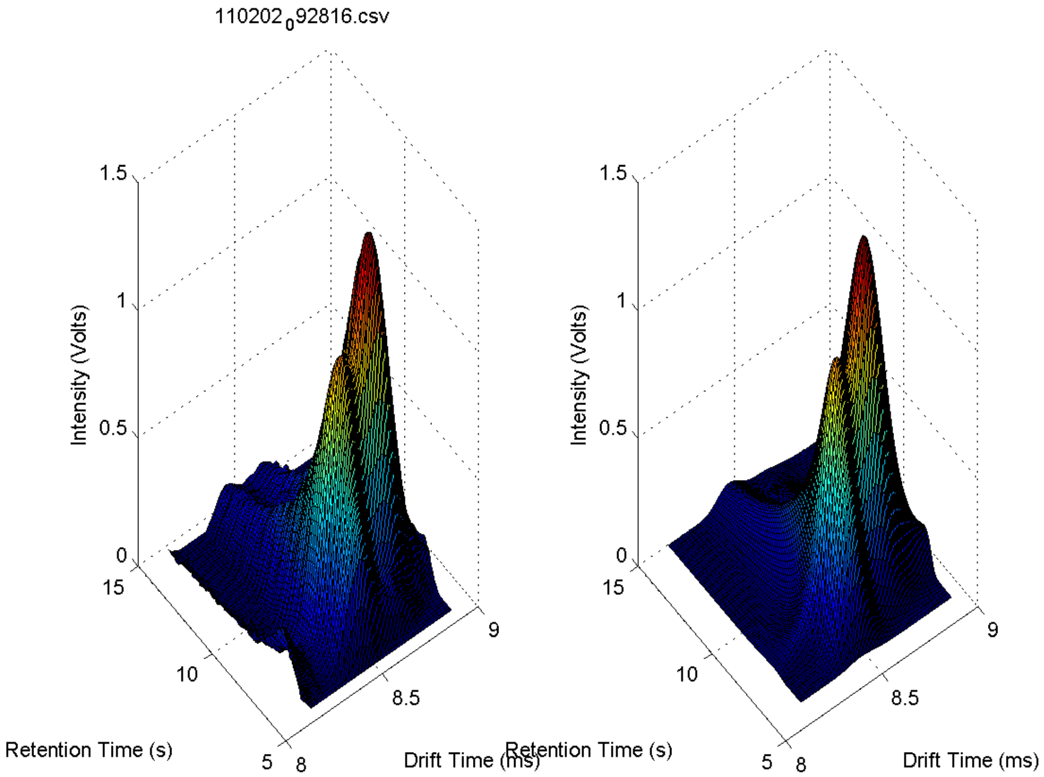
110202$_0$92816.csv
1.5
1
0.5
0
Intensity (Volts)
15
10
5
Retention Time (s)
8
8.5
9
Drift Time (ms)
1.5
1
0.5
0
Intensity (Volts)
15
10
5
Retention Time (s)
8
8.5
9
Drift Time (ms)

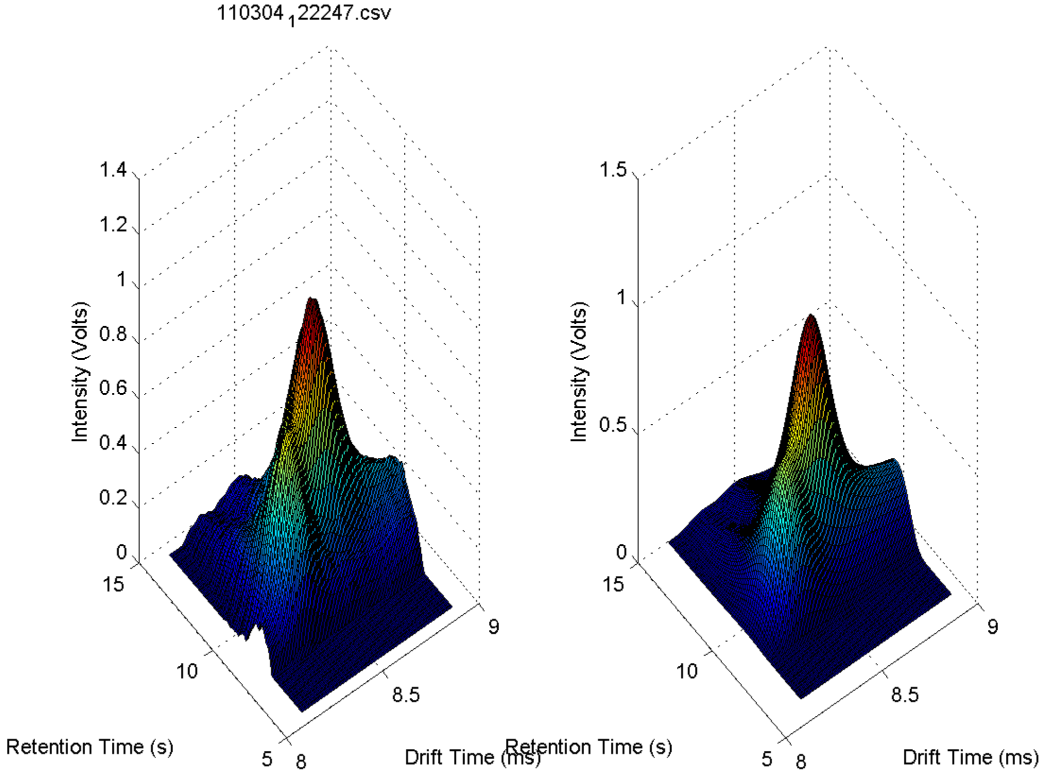
110304$_1$22247.csv
1.4
1.2
1
0.8
0.6
0.4
0.2
0
Intensity (Volts)
15
10
5
Retention Time (s)
8
8.5
9
Drift Time (ms)
1.5
1
0.5
0
Intensity (Volts)
15
10
5
Retention Time (s)
8
8.5
9
Drift Time (ms)

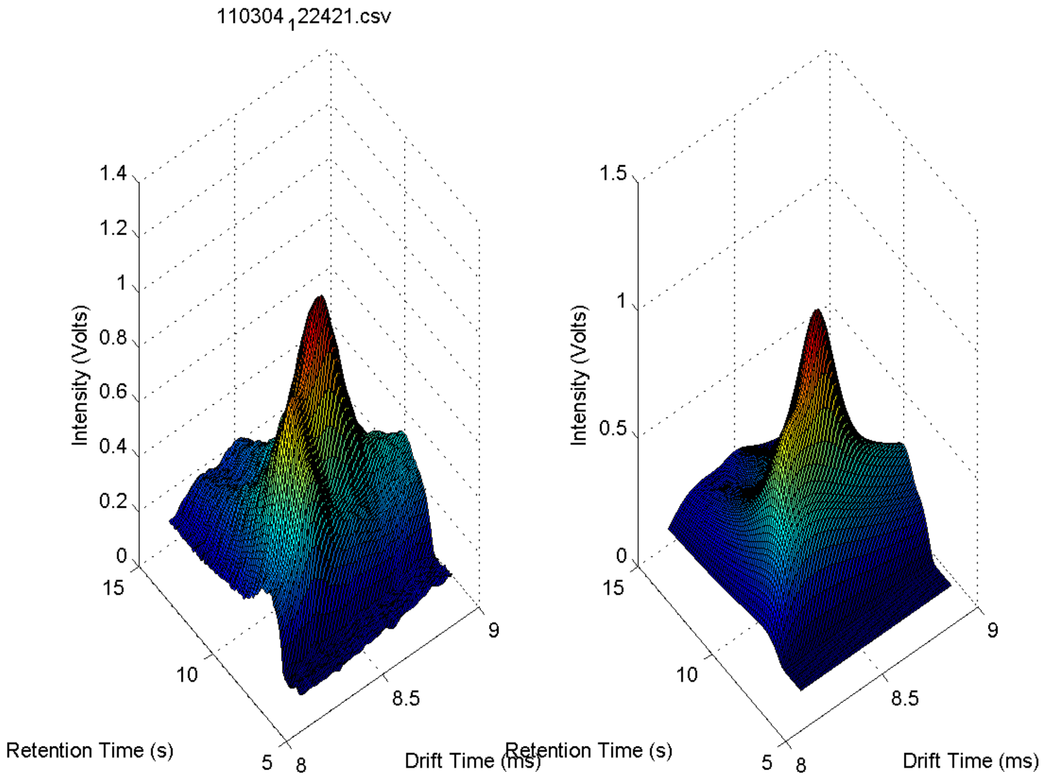
110304$_1$22421.csv
Intensity (Volts)
1.4
1.2
1
0.8
0.6
0.4
0.2
0
15
10
5
8
8.5
9
Retention Time (s)
Drift Time (ms)
Intensity (Volts)
1.5
1
0.5
0
15
10
5
8
8.5
9
Retention Time (s)
Drift Time (ms)

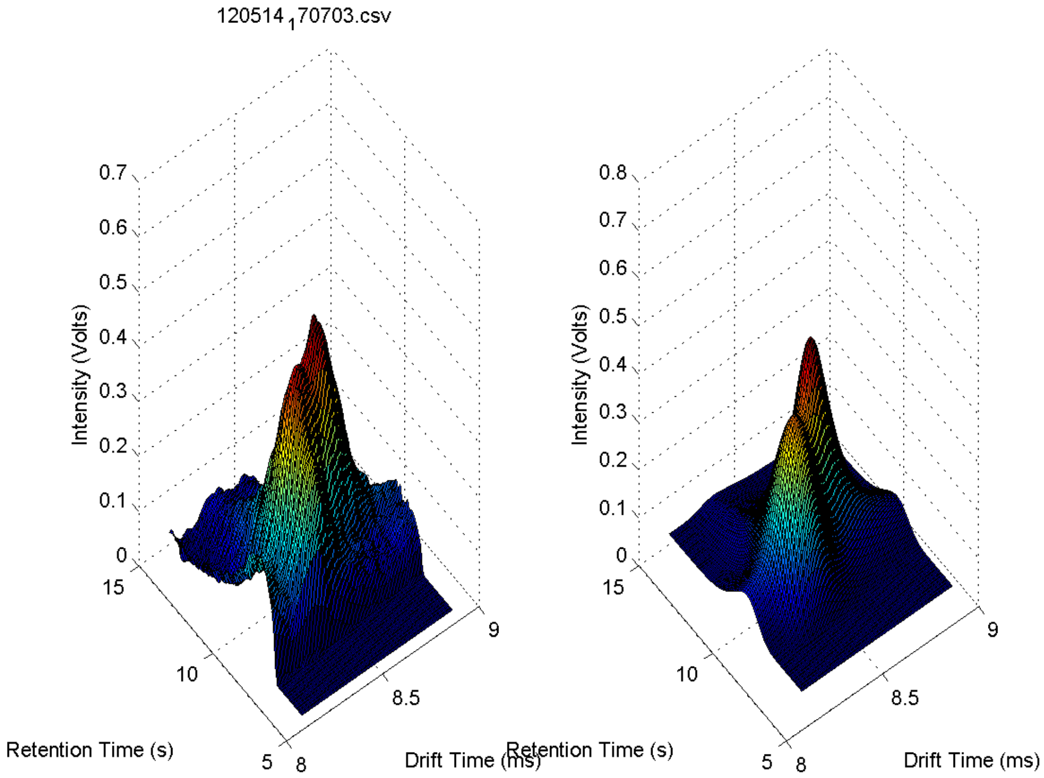
120514$_1$70703.csv
Intensity (Volts)
0.7
0.6
0.5
0.4
0.3
0.2
0.1
0
15
10
5
8
8.5
9
Retention Time (s)
Drift Time (ms)
Intensity (Volts)
0.8
0.7
0.6
0.5
0.4
0.3
0.2
0.1
0
15
10
5
8
8.5
9
Retention Time (s)
Drift Time (ms)

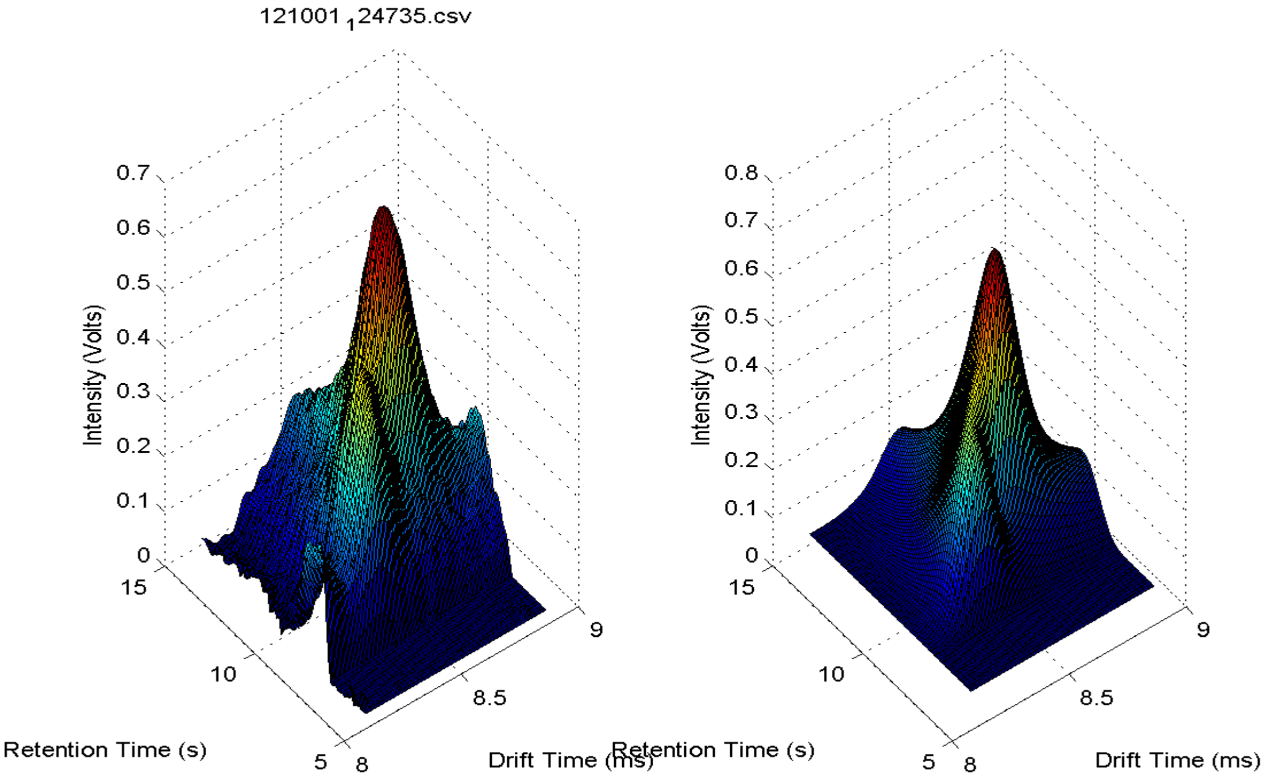
121001$_1$24735.csv
Intensity (Volts)
0.7
0.6
0.5
0.4
0.3
0.2
0.1
0
15
10
5
Retention Time (s)
8
8.5
9
Drift Time (ms)
Intensity (Volts)
0.8
0.7
0.6
0.5
0.4
0.3
0.2
0.1
0
15
10
5
Retention Time (s)
8
8.5
9
Drift Time (ms)

Appendix B

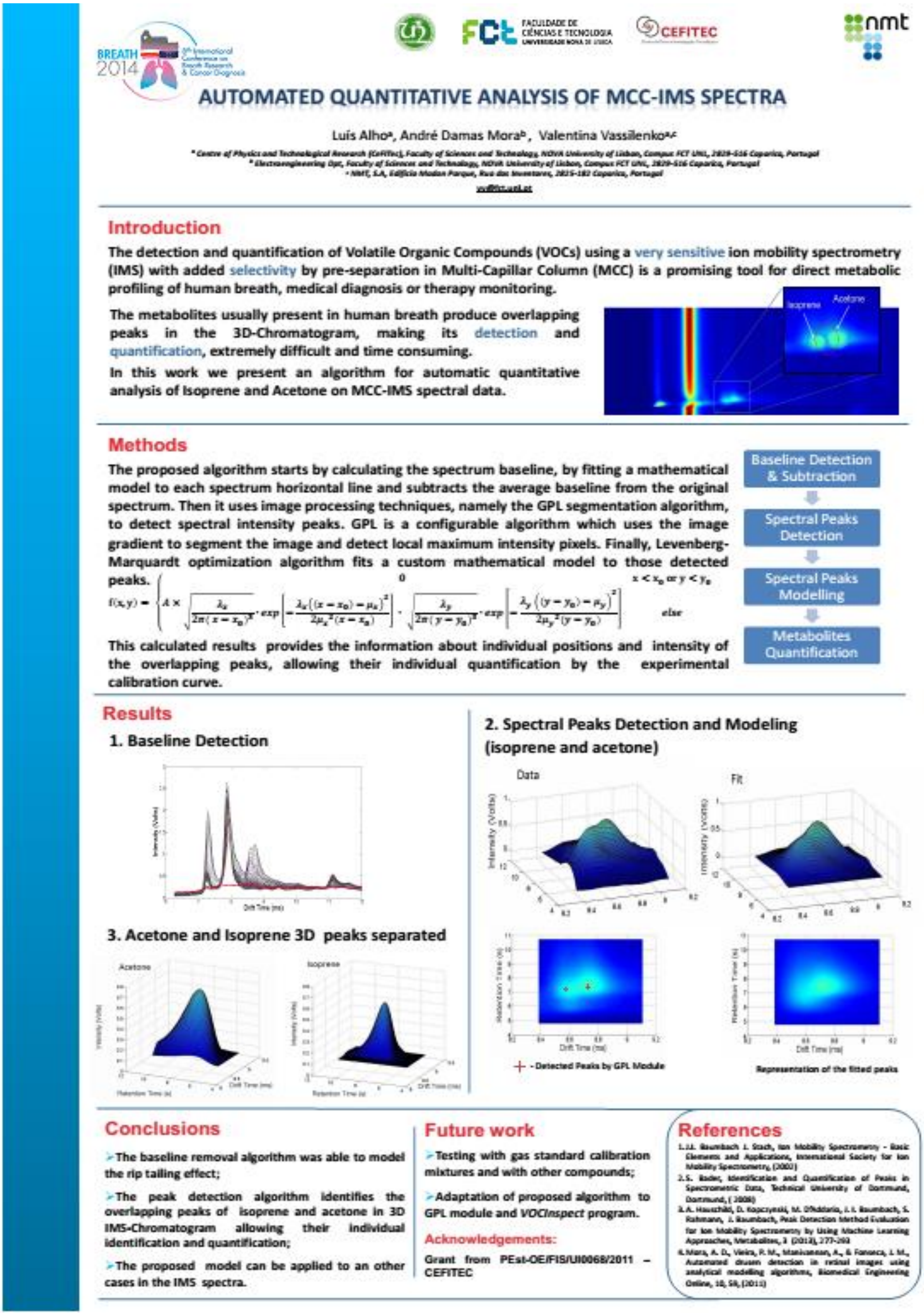

BREATH 2014
8th International Conference on Breath Research & Cancer Diagnosis
FACULDADE DE CIÊNCIAS E TECNOLOGIA UNIVERSIDADE NOVA DE LISBOA
CEFITEC
nmt

AUTOMATED QUANTITATIVE ANALYSIS OF MCC-IMS SPECTRA

Luís Alho[a], André Damas Mora[b], Valentina Vassilenko[a,c]

[a] Centre of Physics and Technological Research (CeFITec), Faculty of Sciences and Technology, NOVA University of Lisbon, Campus FCT UNL, 2829-516 Caparica, Portugal
[b] Electroengineering Dpt, Faculty of Sciences and Technology, NOVA University of Lisbon, Campus FCT UNL, 2829-516 Caparica, Portugal
[c] NMT, S.A, Edifício Madan Parque, Rua dos Inventores, 2825-182 Caparica, Portugal

vv@fct.unl.pt

Introduction

The detection and quantification of Volatile Organic Compounds (VOCs) using a very sensitive ion mobility spectrometry (IMS) with added selectivity by pre-separation in Multi-Capillar Column (MCC) is a promising tool for direct metabolic profiling of human breath, medical diagnosis or therapy monitoring.

The metabolites usually present in human breath produce overlapping peaks in the 3D-Chromatogram, making its detection and quantification, extremely difficult and time consuming.

In this work we present an algorithm for automatic quantitative analysis of Isoprene and Acetone on MCC-IMS spectral data.

Methods

The proposed algorithm starts by calculating the spectrum baseline, by fitting a mathematical model to each spectrum horizontal line and subtracts the average baseline from the original spectrum. Then it uses image processing techniques, namely the GPL segmentation algorithm, to detect spectral intensity peaks. GPL is a configurable algorithm which uses the image gradient to segment the image and detect local maximum intensity pixels. Finally, Levenberg-Marquardt optimization algorithm fits a custom mathematical model to those detected peaks.

$$f(x,y) = \begin{cases} 0 & x < x_0 \text{ or } y < y_0 \\ A \times \sqrt{\frac{\lambda_x}{2\pi(x-x_0)^3}} \cdot exp\left[-\frac{\lambda_x\left((x-x_0)-\mu_x\right)^2}{2\mu_x{}^2(x-x_0)}\right] \cdot \sqrt{\frac{\lambda_y}{2\pi(y-y_0)^3}} \cdot exp\left[-\frac{\lambda_y\left((y-y_0)-\mu_y\right)^2}{2\mu_y{}^2(y-y_0)}\right] & else \end{cases}$$

This calculated results provides the information about individual positions and intensity of the overlapping peaks, allowing their individual quantification by the experimental calibration curve.

Results

1. Baseline Detection

2. Spectral Peaks Detection and Modeling (isoprene and acetone)

+ - Detected Peaks by GPL Module

Representation of the fitted peaks

3. Acetone and Isoprene 3D peaks separated

Conclusions

- The baseline removal algorithm was able to model the rip tailing effect;
- The peak detection algorithm identifies the overlapping peaks of isoprene and acetone in 3D IMS-Chromatogram allowing their individual identification and quantification;
- The proposed model can be applied to an other cases in the IMS spectra.

Future work

- Testing with gas standard calibration mixtures and with other compounds;
- Adaptation of proposed algorithm to GPL module and *VOCInspect* program.

Acknowledgements:

Grant from PEst-OE/FIS/UI0068/2011 – CEFITEC

References

1. J.I. Baumbach J. Stach, Ion Mobility Spectrometry - Basic Elements and Applications, International Society for Ion Mobility Spectrometry, (2002)
2. S. Bader, Identification and Quantification of Peaks in Spectrometric Data, Technical University of Dortmund, Dortmund, (2008)
3. A. Hauschild, D. Kopczynski, M. D'Addario, J.I. Baumbach, S. Rahmann, J. Baumbach, Peak Detection Method Evaluation for Ion Mobility Spectrometry by Using Machine Learning Approaches, Metabolites, 3 (2013), 277-293
4. Mora, A. D., Vieira, P. M., Manivannan, A., & Fonseca, J. M., Automated drusen detection in retinal images using analytical modelling algorithms, Biomedical Engineering Online, 10, 59, (2011)

Appendix C

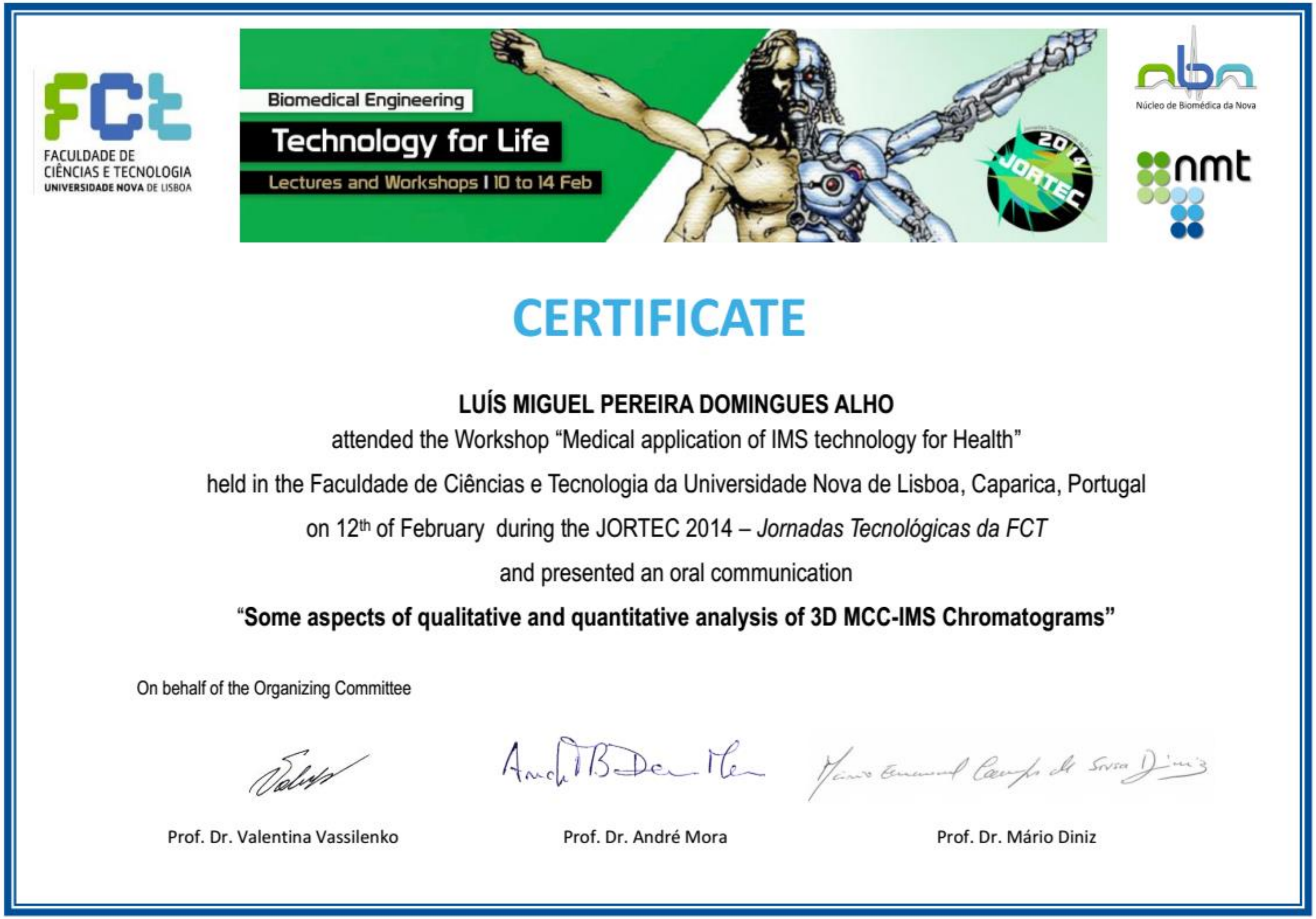
FACULDADE DE CIÊNCIAS E TECNOLOGIA
UNIVERSIDADE NOVA DE LISBOA
Biomedical Engineering
Technology for Life
Lectures and Workshops I 10 to 14 Feb
2014 JORTEC
Núcleo de Biomédica da Nova
nmt

CERTIFICATE

LUÍS MIGUEL PEREIRA DOMINGUES ALHO

attended the Workshop “Medical application of IMS technology for Health”

held in the Faculdade de Ciências e Tecnologia da Universidade Nova de Lisboa, Caparica, Portugal

on 12th of February during the JORTEC 2014 – *Jornadas Tecnológicas da FCT*

and presented an oral communication

“Some aspects of qualitative and quantitative analysis of 3D MCC-IMS Chromatograms”

On behalf of the Organizing Committee

Prof. Dr. Valentina Vassilenko

Prof. Dr. André Mora

Prof. Dr. Mário Diniz